COPPE
Instituto Alberto Luiz Coimbra de Pós-Graduação e Pesquisa de Engenharia
UFRJ

IMPLICATION OF MACROTIDAL COASTAL DYNAMICS FOR SUSTAINABLE USE AND OCCUPATION

Aline Lemos de Freitas

Dissertação de Mestrado apresentada ao Programa de Pós-graduação em Engenharia Oceânica, COPPE, da Universidade Federal do Rio de Janeiro, como parte dos requisitos necessários à obtenção do título de Mestre em Engenharia Oceânica.

Orientadores: Susana Beatriz Vinzón
Fernanda Minikowski Achete

Rio de Janeiro
Julho de 2018

IMPLICATION OF MACROTIDAL COASTAL DYNAMICS FOR SUSTAINABLE USE AND OCCUPATION

Aline Lemos de Freitas

DISSERTAÇÃO SUBMETIDA AO CORPO DOCENTE DO INSTITUTO ALBERTO LUIZ COIMBRA DE PÓS-GRADUAÇÃO E PESQUISA DE ENGENHARIA (COPPE) DA UNIVERSIDADE FEDERAL DO RIO DE JANEIRO COMO PARTE DOS REQUISITOS NECESSÁRIOS PARA A OBTENÇÃO DO GRAU DE MESTRE EM CIÊNCIAS EM ENGENHARIA OCEÂNICA.

Examinada por:

Prof. Susana Beatriz Vinzón, D.Sc.

Dra. Fernanda Minikowski Achete, Ph.D.

Prof. Mário Luiz Gomes Soares, D.Sc.

Prof. Lúcio Silva de Souza, D.Sc.

RIO DE JANEIRO, RJ – BRASIL
JULHO DE 2018

de Freitas, Aline Lemos

Implication of Macrotidal Coastal Dynamics for Sustainable Use and Occupation/Aline Lemos de Freitas. – Rio de Janeiro: UFRJ/COPPE, 2018.

XV, 60 p.: il.; 29, 7cm.

Orientadores: Susana Beatriz Vinzón

Fernanda Minikowski Achete

Dissertação (mestrado) – UFRJ/COPPE/Programa de Engenharia Oceânica, 2018.

Bibliografia: p. 53 – 60.

1. Praias arenosas. 2. Dinâmica costeira. 3. Macromaré. 4. Turismo. 5. Desenvolvimento sustentável. I. Vinzón, Susana Beatriz *et al.* II. Universidade Federal do Rio de Janeiro, COPPE, Programa de Engenharia Oceânica. III. Título.

"It is possible to use natural resources rationally. People have the right to use nature's assets, but not to abuse them"
Perkings Marsh

Agradecimentos

Primeiramente gostaria de agradecer à professora Susana pela orientação e por todas as oportunidades. Pessoa engajada e alegre, fez com que esse projeto fosse possível. Um agradecimento especial à Fernanda pela co-orientação, mesmo depois do nascimento do Caio, agradeço demais!

Aos companheiros de turma: Leo, Igor, Bruno, Vivi, Aline. A companhia de vocês adicionou leveza ao período de matérias! À Lara e à Luana, um agradecimento especial pelos momentos, risadas, viagens e companhias no longo trajeto casa-fundão. Ao Douglas Medeiros e ao Pedro Paulo, pelas discussões altamente produtivas no nosso grupo de python, toda troca de experiências e de rotinas que eu vou levar pra sempre.

Ao pessoal do LDSC: Laíssa, Ernesto, Gabi, Ju, Luiz, Paloma pela companhia no laboratório e nos almoços e por agregar conhecimento em diversas etapas desse trabalho. Um obrigada especial à Pati que me auxiliou em todos os momentos que precisei, me salvando várias vezes no ArcGis e com as imagens de satélite.

Agradeço também ao Douglas Nemes pela orientação nos trabalhos de campo em Salinas e pelas medições realizadas. E também não poderia deixar de agradecer à Monique e ao Natan por me receberem em casa e me mostrarem um pouco mais de Salinas. Me encantei pelo lugar e nunca fui tão bem recebida! Muito obrigada!

Ao grupo do LiOc: Izabel, Henrique, Pedro, Júlia e Guilherme. Muito obrigada por dedicar o tempo de vocês sempre que eu precisei de uma ajuda!

Aos professores Afonso e Marcos por me deixar ainda mais encantada com o mundo da oceanografia física e por nos guiar nos primeiros passos do mestrado.

Ao grupo do CENPES, que mesmo "longe" continuaram marcados pela presença nos dois anos que antecederam esse trabalho. Nenhum grupo vai ser tão feliz quanto o de vocês e obrigada pelo processo de brotherização!! Um agradecimento especial ao Renato, ao Guerra, ao Wellington e ao Luis Manoel que foram meus orientadores de vida mesmo antes de entrar pro mestrado.

Aos meus pais, que apesar de sentirem minha falta, sempre me apoiaram a seguir esse caminho e desbravar os oceanos. Aos meus avós queridos, que sempre se espantavam quando eu dizia que ainda estava indo ao fundão e que o trabalho ainda não tinha terminado. Morri de saudades de vocês nesses últimos meses! À

maletinha da minha irmã que, apesar de todas as brigas, mora no meu coração! e que passou a me fazer companhia em casa no último mês. E um agradecimento especial ao Pedro que também foi um ótimo orientador nas horas vagas, meu maior companheiro e apoio ao longo de todos esses anos!

Resumo da Dissertação apresentada à COPPE/UFRJ como parte dos requisitos necessários para a obtenção do grau de Mestre em Ciências (M.Sc.)

IMPLICAÇÕES DE DINÂMICA COSTEIRA DE MACROMARÉ SOBRE O USO E OCUPAÇÃO SUSTENTÁVEIS

Aline Lemos de Freitas

Julho/2018

Orientadores: Susana Beatriz Vinzón
Fernanda Minikowski Achete

Programa: Engenharia Oceânica

O município de Salinópolis no estado do Pará, é um exemplo de área costeira que se desenvolve de forma desordenada, com atividade turística concentrada no mês de julho gerando uma exploração agressiva dos recursos naturais locais. Apesar do alto potencial turístico da região para atividades esportivas e ecológicas, atualmente o turismo é baseado principalmente no uso da praia para recreação. O principal objetivo deste estudo é compreender a dinâmica natural de Salinópolis (clima de onda e meteorologia e variações na linha de costa) a fim de proporcionar uma melhor estratégia de desenvolvimento das atividades turísticas para a região. Os resultados mostram uma variação sazonal do clima de ondas com maiores alturas (0.8 m com direção N-NE) no primeiro semestre. A intensidade do vento é maior durante o segundo semestre e coincide com a estação seca. A direção principal do vento é paralela à costa, criando condições perfeitas para a prática de kitesurf e outros esportes de vela. O conhecimento da direção do vento permite também o desenvolvimento de um projeto otimizado de passarelas pelo mangue na área da cidade adjacente à praia do Maçarico. A passarela inclui múltiplas funções dentre elas a melhoraria na circulação de vento no centro da cidade e como ferramenta de educação ambiental para moradores e turistas. Na área sob erosão, rua da Frente, a instalação de barreiras permeáveis possibilitariam a deposição de sedimento, contendo o processo erosivo.

Abstract of Dissertation presented to COPPE/UFRJ as a partial fulfillment of the requirements for the degree of Master of Science (M.Sc.)

IMPLICATION OF MACROTIDAL COASTAL DYNAMICS FOR SUSTAINABLE USE AND OCCUPATION

Aline Lemos de Freitas

July/2018

Advisors: Susana Beatriz Vinzón
Fernanda Minikowski Achete

Department: Ocean Engineering

Salinópolis, a brazilian city at Pará state, is an example of a coastal area under unorganized development with social and environmental impacts. Tourist activity in the city leads to an unsustainable development and an aggressive exploration of the local resources due to its high seasonality. Despite the region potentiality, tourism is based only on beach use for recreation. The main goal of this study is to understand the natural dynamic of the system (wind, rain and waves season and morphological changes) in order to provide a better development strategy of tourist activities for the region of Salinópolis - PA. Results show that wave climate has a seasonal variation with higher waves in the first semester. This condition is favorable for surf practice. Wind intensity is higher during the last semester and coincides with the dry season. Wind direction is parallel to the coast, the perfect condition for windsurfing, kitesurfing and sailing. Wind direction knowledge also permits the development of a better design for the mangrove walkway at Maçarico beach. A walkway parallel to the main wind direction would improve airing at the city center. Mangrove walkways would act as an education tool for residents and tourists. Mangroves would also work as coastal protection near the secondary access where the erosion threatens the parking area. The installation of permeable dams allow the deposition of sediment to stop erosion.

Contents

List of Figures

List of Tables

Chapter 1

Introduction

The coastal zone represents the land and sea interface. It has a dynamic characteristic as waves, winds and tides forces coastal morphology [1]. Coastal zones are very important economically. Almost 30% of the global population [2–4] live by the shore and tropical coasts are particularly attractive for tourism [5, 6].

Coastal zones are in constant conflict induced by economic development pressure. They often demands stability and natural processes may cause continuous changes [7]. The development pressure is observable in crowded beaches and in the amount of seaside infrastructures. These structures, in many cases, destroy the aesthetic value that originally drew people to the coast [8]. The existing conflict becomes more evident when erosion impacts coastal infrastructures or when accretion make a beach too wide for walking to the waterline [1].

In developing countries, coastal activities place additional pressure on the natural resources [5, 6]. Impacts on precarious infrastructure can be observed, such as overuse of water resources, pollution by sewage and littering as well as disorganized development of the city [5]. The unsustainable use and unrestricted development of the coastal areas are the major cause of the problems that are now encountered worldwide [1]. Knowing local dynamics is indispensable in order to avoid future irreversible damages to the environment.

Coastal areas are particularly attractive for tourism, one of the largest industry of the 21st century [5, 6]. Visitors usually search for beach scenic views, wildlife, pleasantly warm temperatures and good food. But surveys indicate that the most important factors in attracting visitors, besides the landscape, are safety; easy access and infrastructure [9]. The activity brings economic benefits through hotel and restaurant expenses and other tourism-related services but, without a proper management, it overexploits on natural resources and the local community.

Tourism can change from an economic solution to an environmental problem as seen in several places in the world. For instance, in Mallorca, Spain, mass tourism had led to overcrowded beaches, strong pressure over water resource and massive

construction on the coastal zone - with coastline retraction as consequence [10]; in Antigua, West Indies, ecosystems have been severely degraded as a result of tourism development [11]; in Wadden Sea, The Netherlands, tidal flats - designated as UNESCO World Heritage - have their ecological balance threaten by the increase of tourists and the economic pressure [12]; in Venice, Italy, the city attracted 40 visitors for every inhabitant, by the time of 2005, and consequences range from littering to overcrowding [13].

Salinópolis, a Brazilian city in Pará State, is an example of a coastal area under disorganized development with consequent social and environmental impacts [14–16]. Salinópolis, also called Salinas, is located at 00°36'49" S 47°21'22" O (Fig. 1.1). At a distance of 220 km from the state capital Belém, it has a population of 39.328 inhabitants [17]. Tourism and fishery are the basic economic activities, Salinas is one of the most popular vacation places in Pará. Tourism activities are highly seasonal, receiving about 10 times its population during weekends in July [18], month of school holidays.

A study from the Salinópolis government indicates that 94.25% of the visitors had the natural beauty as the main factor for their staying that last on average 6.5 days. Only 10.2% of the visitors stay in hotels and the majority stays in relatives' home or rented houses. However, the major expense of visitors is with accommodation (R$48 per person per day) followed by feeding (R$28.50), transport (R$14.50) and souvenirs (R$7.80). Only 8.7% of the visitors spend their time in Salinópolis practicing sports and the majority of visitors (89.4%) spend their time with recreational and resting activities. 25.8% of the tourist are from Pará. São Paulo (17.5%) and Rio de Janeiro (8.6%) are the second and third biggest group [19].

Salinas has four major beaches (Fig. 1.1): Atalaia at the east area, Farol Velho at the central area, Maçarico and Corvina at the west area. City development started closer to Maçarico and Corvina beaches and those were historically the most visited ones. More recently (end of 1990 decade), an urbanization project built a promenade with kiosk and a parking area close to Maçarico and Corvina.

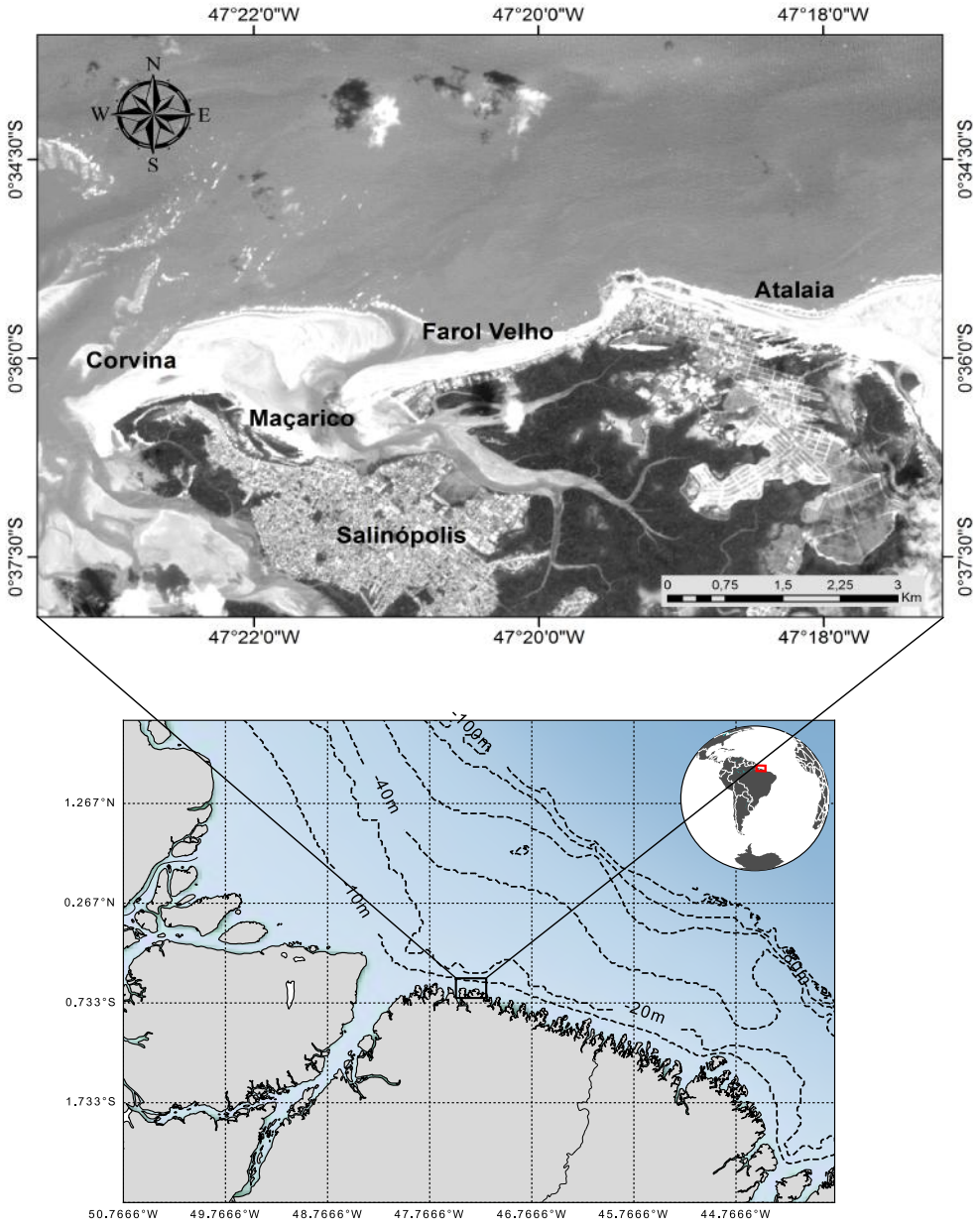

Figure 1.1: Location of the city of Salinópolis - PA - and its main beaches. The small globe indicates the location of Pará coast in South América; the lower portion of the figure shows Salinópolis location on Pará coast and the upper figure shows the location of main beaches in Salinópolis.

The project included some beach access, part of the built concrete infrastructure: a walkway that leads out to the central area of the Corvina beach and some other access from the promenade. The access were meant for pedestrian, having the parking lot close by (Fig. 1.2.a). After the construction of the promenade, the beach growth, following the general coast dynamics; a mangrove forest developed in front of the promenade, with an extension of 100 to 300 meters, restricting the

beach access. In 2017, a walkway to the beach was built in wood, at the beginning of Maçarico beach (Fig. 1.2.b)

Progressively, tourism had migrated to Atalaia and Farol Velho beaches, where car access is possible and allowed. This change may has been driven by the lack of access to the beach at Maçarico, the lack of infrastructure (the kiosks along the promenade were closing as the beach lost the occupation) and the construction of a bridge that make the access to Atalaia beach easier.

Cliffs are common features in the area. Part of the city, built on top of such cliffs, was severely exposed to erosion in the past (Rua da Frente). As a result, a seawall was built as an attempt to stop the erosion process but it ended up being destroyed. The area is next to Maçarico beach (Fig. 1.3) and the waves that reach the coast reflect on the remainders of the seawall. The cliff is under risk of landslip.

Considering the importance of turism for Salinópolis, the region dynamics and the consequences of this dynamics on coastal infrastructure and activities, this work aims to present a physical characterization of Maçarico and Corvina beaches, the main forcing and major processes governing their dynamics. We focused on Maçarico and Corvina since those are well-preserved, under threat, areas with a diversity of environments, as mangrove forests, beaches and estuaries. It may offer other tourism development options, exploring its potential for sports, ecotourism, gastronomic and cultural tourism, adding value to the already popular "Sun and Beach" tourism. Actions towards those alternatives may help for a more sustainable tourism development, breaking the extreme seasonality nowadays occurring.

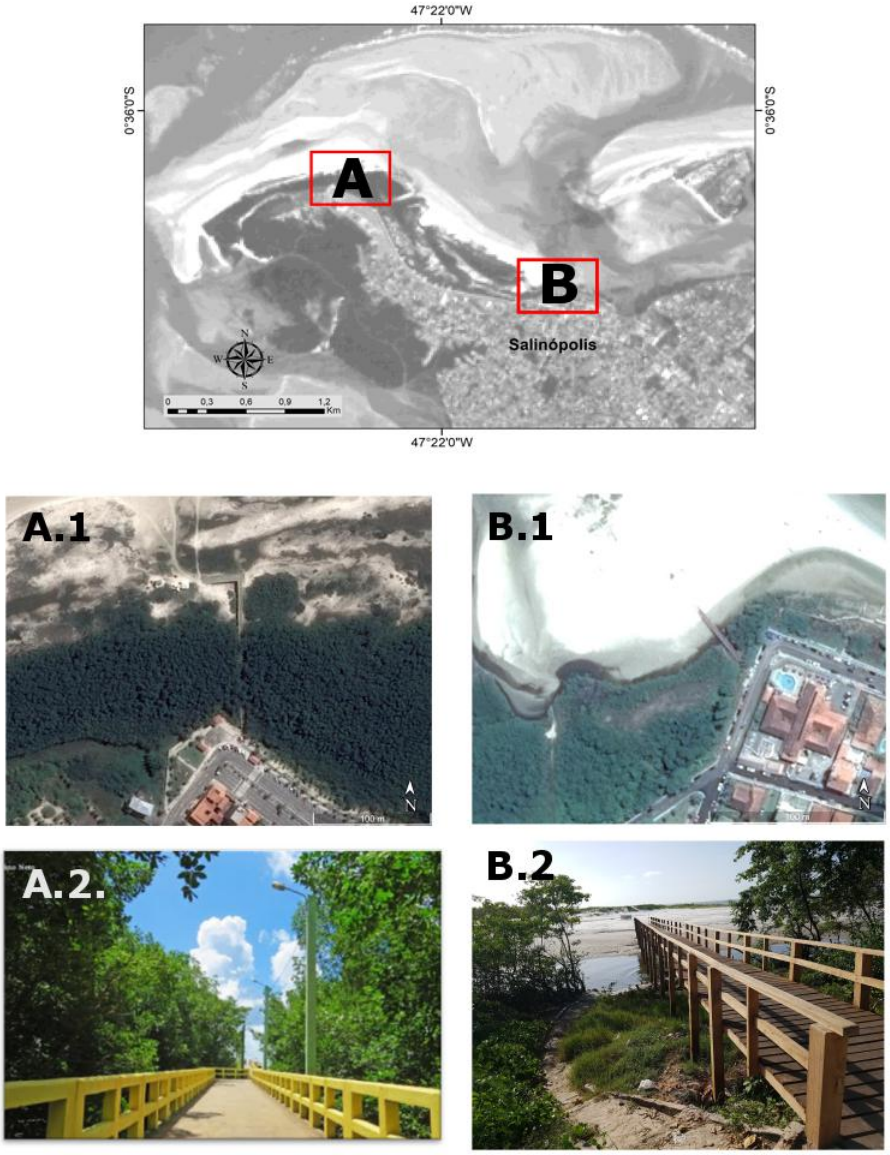

Figure 1.2: Location of the two access to the Corvina and Maçarico beaches (A, B, A.1 and A.2). The red squares represent the location of the zoom images A.1 and B.1; images A.2 and B.2 are pictures from the local. A.2. shows the concrete walkway and B.2. is the walkway made of wood for accessing Maçarico beach

Figure 1.3: Photographs from the isolated area of the cliff and warning signs (photos A and B) and from the remaining of the seawall (photos C and D).

1.1 Objective

The main goal of this study is to understand the natural dynamic of the region (wind, rainfall, waves, tides and morphological changes) in order to provide a better development strategy of tourist activities for the region of Salinópolis - PA. To achieve this objective, we defined four specific objectives:

- Characterize the area in terms of its forcing (rainfall, wind, waves and tide);
- Define erosion/accretion pattern and shoreline changes;
- Propose activities for a better use of the natural resources;
- Propose infrastructures interventions that agree with the local dynamic.

Chapter 2

State of Art

This chapter presents the state of art of the natural dynamics of Salinópolis.

2.1 Atmospheric Forcing: Winds and Rainfall

The Brazilian North and Northeast regions are under influence of the Trade Winds throughout the year. These winds blow from Northeast in the Northern Hemisphere (NH) and Southeast in the Southern Hemisphere (SH). The Intertropical Convergence Zone (ITCZ) is the region where the trade winds converge due to a low-pressure near the Earth's Equator. It has a North-South seasonal shift reaching its Northernmost (14° N) position during austral late winter and early spring, and the southernmost position (5° S) usually occurs during austral late summer and early fall [20]. ITCZ migration is controlled by the Sea Surface Temperature Anomaly (SST_a) and by the intensity of both Atlantic high-pressure centers [21, 22]. In September and October (early spring, SH) wind intensity at the Brazilian North coast is higher due to Southeast Trade Winds contribution and weaker in March and May [23]. SOUSA [24] observed wind speed above 8 $m.s^{-1}$ from January to March and a mean wind speed of 5 $m.s^{-1}$ in July.

Interannual variation also occurs in trade winds due to El-Niño Southern Oscillation (ENSO), periodic anomalies from expected sea surface temperatures (SSTs) in the equatorial Pacific Ocean. These ocean temperatures anomalies can affect weather patterns around the world by influencing high and low pressure systems, altering winds, and precipitation [25].

The Northern part of Pará state is characterized by a well-defined rainfall climate. ITCZ migration is the primary regulator of it. As a consequence, rainfall follows both seasonal and interannual variation of the ITCZ. The wet season is from December to May, when we have most of the annual rain volume and a dry season is from June to November [26]. The velocity of ITCZ migration back to the Northernmost position defines the amount of rain for the Brazilian Northern coast [21, 22] and

El-Niño affects rain climate decreasing the amount of rain for the period [26].

2.2 Tides and Coastal Currents

Salinópolis has a macro-tidal semidiurnal regime with a mean tidal amplitude of 4.82 meters in spring tide and 2.64 meters in neap tide [27].

Higher level range (>5m) might be seen in March and April due to wet season and spring equinox [28]. Rapid water level variation of few meters results in significant tidal currents reaching 0.5 $m.s^{-1}$ and plays an important role in morphological changes [29]. Higher current values at Salinópolis occurs during the East and West portions due to the presence of tidal channels. The highest current intensity occurred during flood tide in the East portion (0.58 $m.s^{-1}$). The lowest values occurred at the Corvina beach where currents range from 0.15 $m.s^{-1}$ during the flood and 0.25 $m.s^{-1}$ during the ebb [30].

During ebb tide, the longshore current is toward West and currents invert its direction during the flood tide. At the central portion of Farol Velho and Atalaia the longshore currents are toward West during the entire tidal cycle [30].

2.3 Wave and Tidal Modulation

The macro-tidal regime is also responsible for wave modulation at the Salinópolis coast [31]. The wave climate at a shoreline depends on the offshore wave climate and on the bottom topography that modifies the waves as they travel shoreward [32]. The presence of submerged sandbanks induces wave break away from the coast, reducing the energy that reaches the coast [33]. Therefore, lower waves with shorter periods are observed during low tide because of sandbanks protection. On the other hand, bigger waves reach the coastline with the increase of depth at high tide. The effect of wave modulation is more evident at sheltered beaches where tidal energy is higher than wave energy [31].

ERA-INTERIM time series of a point off Pará coast (3°N, 45.75°W) evidence a seasonal pattern on wave climate. From December to May it shows higher wave height (about 3 meters) and wave period (12 seconds) coming from North. From June to November, wave height and period decrease (up tp 2 meters and an average of 8 seconds) and wave direction increases (waves from East, reaching about 100°). Measured data, from 2011 to 2012, in a water depth of 20 meters show wave height reaching the highest mean value in February and March 2012 (2.27 m and 2.14 m respectively) [24]. The highest peak period was observed in November 2011 (with a mean value of 9.85 s) and in May 2012 (9.40 s). In May, wave direction also reached

its lowest mean value (50°) indicating a Northeast wave direction. October was the month with higher wave direction (124°), with a southeast component [24].

PEREIRA *et al.* [31] registered this seasonal variation by the coast of Pará. Higher wave height (1.1 to 1.5 m) with wave direction between 35° and 50° were observed in March 2009. During September and October of the same year, wave heights were lower (1 to 1.2 m) with direction from 65° to 85° [31]. Peak period varies from 2 to 12 s with the higher peak period during flood tide, especially in the afternoon when associated with stronger winds [28]. Wave parameters also vary among the beaches, with lower wave period (4.20 to 4.10 s on April and 4.20 to 4.40 s on October) and wave heights (0.44 to 0.63 m on April and 0.60 to 0.65 m on October) at Corvina and Maçarico [28].

FISCH [34] highlights the arrival of storm waves from the North Atlantic Ocean at Brazilian northeast coast. The swell has a maximum period of 24 seconds and wave height of 1.5 to 2.0 meters at Ceará coast. Those events have enough energy to destroy coastal structures [34]. Part of these waves energy might also reach Pará coast due to its geographical orientation as shown by ERA-INTERIM outputs with North direction waves at a point off Pará coast.

2.4 Morphological Changes

RANIERI [28] describes the morphodynamics of the Salinópolis beaches from 1988 to 2013. The study shows punctual areas of erosion as at the center portion of Atalaia beach and an accretive area at the east part of this beach. The residual sediment transport direction is from east to west [28, 35].

At the west portion of Salinópolis, Maçarico and Corvina beaches shows an accretion pattern although RANIERI [28] observed a decrease in variation rate of the mean coastline from 2001 on. This portion presented the higher sediment load [28] where is observed the major accretive area. Accretion occurs due to the estuaries dynamics which present tidal channels with ebb tidal deltas supplying Maçarico and Corvina with sediment [28, 35]. Another possible cause for the deposition according to RANIERI [28] is the maintenance of the vegetation that has the capacity to trap sediments; and the lower anthropic impacts in the coastline compared to Atalaia and Farol Velho.

Seasonal changes on punctual beach profiles are also observed, with dry season presenting an accretion pattern compared with wet season [28, 36]. The highest sediment load is still observed at Corvina and Maçarico beaches [28].

2.4.1 Mangrove forest at Maçarico and Corvina

Salinópolis local population traditionally constitutes from artisan fishermen that have a simpler lifestyle. They depend on natural resources for their living [37] and fishery activity is directly related to mangrove preservation.

At Maçarico and Corvina beaches, the whole orla is occupied by mangroves which comprises an area of about 1 km^2. Species of *Avicennia* (*A. germinans*, *A. schaueriana*), *Rhizophora* (*R. mangle*, *R. racemosa*), *Laguncularia racemosa* and *Conocarpus erectus* are found in Salinópolis area [38]. The presence of those trees protects the shore against the erosive process that is less perceived by the population at this portion of Salinópolis compared to Farol Velho and Atalaia. Few studies were undertaken considering the mangrove at Maçarico and Corvina and precise information about species composition and total area are not available. The ones that exist focus on anthropogenic impacts as littering and sewage disposal [16, 39]. RANIERI e EL-ROBRINI [40] presents the evolution of the shoreline, based on vegetation limits, after the promenade construction. ASSUNÇÃO *et al.* [41] shows the mangrove development as a problem since it restricts beach access.

2.5 Use and Occupation at Salinópolis

From 1990 decade public urbanization projects started building an image of the city in order to attract tourist from inside and outside the country [14]. An example is the complex of Maçarico Orla (with kiosks, restaurants and a parking lot) were a series of music festivals are promoted during the high season. However, those projects do not concern social and environmental impacts. Music festivals presented has no cultural relation with local community and intensify the overcrowd of the city as it happen during high season [14].

Salinópolis' economy depends on tourism. During low season it turns into a "city of ghosts" and local community that depends on tourism stays unemployed. During high season, city infrastructures as water distribution, sewerage and garbage collection are overused and inefficient [14].

The lack of efficient infrastructure reflects on garbage and sewer disposal on beaches and mangroves forest [16]. Consequences range from beach and underwater pollution to aesthetic and economic problems with indirect impact on tourism [14, 16]. Infrastructures investments are not efficient due to the seasonal pattern of tourism, being underused during most part of the year. This leads to an unsustainable use of the natural resources.

Chapter 3

Methodology

This chapter presents the available data and the methodology applied in its treatment. Some considerations were used for general data:

- Wind and wave direction are defined from their origin (coming from);
- Currents direction are towards;
- Nautical notation was used, starting at 0° on the upper portion of the directional rose as geographical North representative;
- Directional angle increase clockwise with East represented by 90°; South by 180°; 270° at West and 360° back at North;
- Geographical directions was considered and magnetic declination were used for data correction when necessary.

3.1 Data Analysis and Acquisition

3.1.1 Wind

Wind intensity and direction were obtained from the Brazilian National Meteorological Institute (INMET wepage) [1]. Hourly data for an eight years period (from 1 January 2009 to 31 December 2016) was analyzed. The station is located at 00° 37'S and 47° 21'W (Fig. 3.1), in the city center of Salinópolis, at 21 meters high.

Wind direction was divided into the 8 main directional categories every 45° (North, Northeast, East, Southeast, South, Southwest, West and Northwest) (More in section 4.1). Measurements date and time were converted to local zone.

We used Python scripts for data analysis. Measurements were grouped by month and by directional categories to estimate their frequency of occurrence. Box plots

[1] `http://www.inmet.gov.br/projetos/rede/pesquisa/`

were used to analyze wind speed distribution along the day hours and along the year.

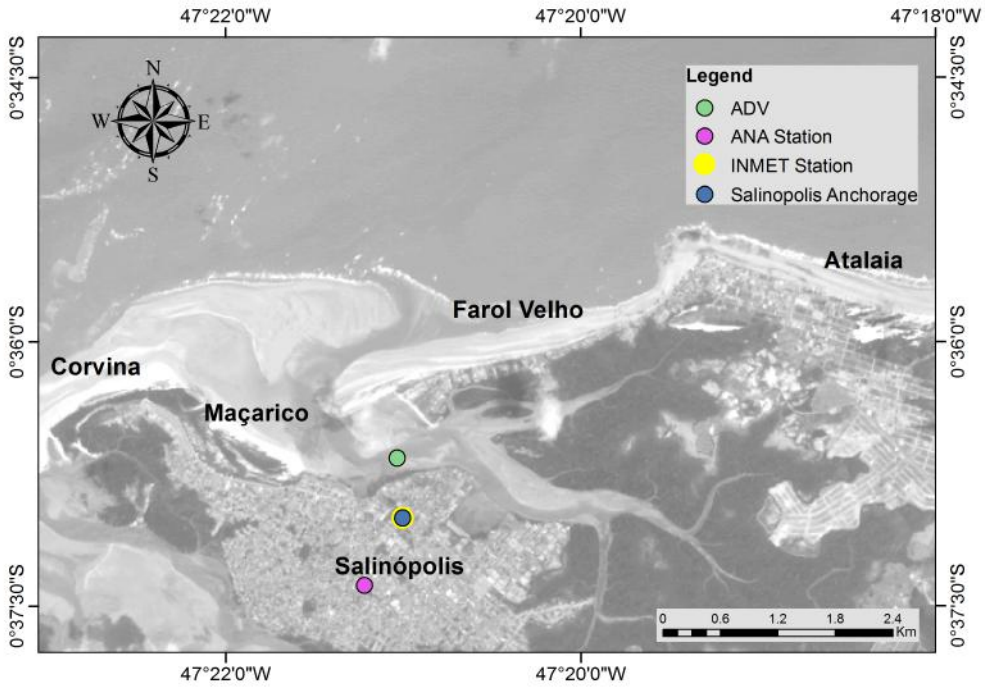

Figure 3.1: Location of observation: INMET station (yellow circle); ANA station (pink circle); navy Salinópolis anchorage (blue circle) and ADV measurement position (green circle)

3.1.2 Rainfall

A timeseries of thirty-seven years of daily rainfall was obtained from the Brazilian National Water Agency (ANA), starting on 1 January 1978 to 31 December 2015. Data retrieved from the Hidroweb page [2] of the station 47002 located at Salinópolis city center (00°37'23" S and 47°21'13" W).

Additionally, hourly rainfall dataset of 8 years, between 2009 and 2016, was obtained from INMET and used for assessing the distribution along the day. Both stations ANA and INMET stations are located at Salin´opolis city center according to institutional information (Fig. 3.1).

Python scrips were used for rainfall analysis. From the ANA dataset we calculated precipitation climatology, dividing the year in three main seasons: wet (January to May); Transitional (December, June and July) and Dry (August to

[2] `http://www.snirh.gov.br/hidroweb/publico/medicoes_historicas_abas.jsf`

November). Month mean, maximum and minimum volumes were calculated. The number of rainy days per month were also calculated using ANA dataseries.

INMET data were used for daily distributions. The mean volume of rainfall per hour were calculated. Since the number of days without a considerable rain volume is elevated during transitional and dry season, calculations of average scenario for the rain distribution along the day only consider registers with values higher than 0.2 mm.

3.1.3 Tidal Currents Measurements

An ADV (Acoustic Doppler Velocity) was used for currents measurement on the tidal channel located between Corvina and Farol Velho at 0°36'39.6576" S, 47°21'1.872" W (Fig. 3.1). It was a short, preliminary measurement of a few days at the end of a spring tidal cycle (22 November 2017 to 25 November 2017) divided into two periods. The first timeseries of 23 hours started on 22 November 2017 at 2:48 PM and ended on 23 November 2017 at 3:48 PM with a sampling rate of 4Hz. The second acquisition of 52 hours and 30 minutes started on 23 November 2017 at 5:30 PM and ended on 25 November 2017 at 10:03 PM. Sampling rate set was 2 Hz. The instrument was placed in a frame and rest 90 cm from the channel bottom. The equipment got emerged during low tide and a pressure limit of 50 cm was set as "dry condition" for a better data consistency. Data was filtered with a 5 minutes window average, considered appropriated for tidal analysis. Current data measurement was planned to be a first approach on tidal currents. Those measurements aims to provide information about currents magnitude and direction at the channel between Maçarico and Farol Velho.

3.1.4 Remote Sensing and Vegetation Line Analysis

Landsat 8 images from 2013 to 2018 were used for vegetation line growth/reduction analysis. Landsat 8 has a revisit interval of 16 days and spatial resolution of 30 meters. Cloud cover is persistent at Pará coast due to the ITCZ influence. Images choice were based on low cloud cover over Maçarico and Corvina shoreline (Tab. 3.1). Although it has low resolution, Landsat 8 were used because of its revisit internal and the number of images per year. The boundary between vegetation and beach sand were defined as boundary. To enhance these limits, a band composition for false color and vegetation analysis was performed as shown in table 3.2 [3].

[3] https://blogs.esri.com/esri/arcgis/2013/07/24/band-combinations-for-landsat-8/

Table 3.1: Landsat 8 images date, resolution and cloud cover situation

Date	Satelite	Resolution	Cloud cover
31/10/2013	Landsat 8	30 m	Low
08/12/2015	Landsat 8	30 m	Low
29/12/2017	Landsat 8	30 m	Low
15/02/2018	Landsat 8	30 m	Low

Table 3.2: Landsat 8 Composite bands and the feature limit to be enhanced[3].

Feature highlighted	Band combination as RGB
False Color (urban)	7 6 4
Vegetation Analysis	6 5 4
Land/Water	5 6 4
Natural Color	4 3 2

The Digital Shoreline Analysis System (DSAS) was used for coastline changes statistical calculation [42]. DSAS is freely available on Esri ArcGIS[4]. With DSAS, users are able to calculate shoreline rate-of-change from multiple historic shorelines. We defined a shoreline for each satellite image based on vegetation limits.

The use of the low tidal line as coastline definition was very imprecise at Salinópolis due to its macrotidal regime and the sandbank dynamics of the region. Mangroves are at an elevated part of the beach flooded by tidal channels. As the beach grows, mangrove forest advances. Thus, the vegetation was used as a more accurate parameter for the advance or retreat of the beach.

A baseline was set for the application of normal transects that crosses each of those shorelines. The distance between them is used for the statistical calculation of the vegetation evolution. In order to compare with RANIERI [28] results the same available calculations at DSAS toolbox was used: the Net Shoreline Movement (NSM) which reports the total distance between the oldest and most recent shorelines for each transect; and the rate of the shoreline movement, named End Point Rate (EPR). The EPR is calculated by dividing the distance of the total shoreline movement by the time elapsed between the oldest and the most recent shoreline [42].

[4] `https://woodshole.er.usgs.gov/project-pages/DSAS/`

3.2 Hydrodynamic and Wave Model

ERA-Interim is a reanalysis of the global atmosphere parameters available from 1979. Reanalysis is a combination of model information and observations to produce a consistent best estimate of atmospheric, wave and oceanographic parameters [43]. ERA-Interim is a global wave model with coarse resolution that shows good results for deep water but not as reliable in coastal areas.

Information on the wave climate by the Salinópolis shore is sparse (model or measurement), thus a hydrodynamic model coupled with a wave model was used to propagate ERA-Interim offshore wave to shallow water.

Annual mean and standard deviation were calculated from the ERA-Interim time series in order to select a representative period for the model application (Tab. 3.3). This model simulation aims to provide a base scenario for wave climate in a regular year. A period from 1 June 2010, to 31 August 2011 was chosen as it corresponds to wave parameters closest to the mean. The availability of data for model validation in 2011, described in section 3.2.2, were also considered.

Table 3.3: Mean wave parameters from the ERA-INTERIM output for the choice of a simulation period. Values are representative for the first (left table) or the last (right table) semester. Colors represent values close (yellow), above (red) and under (green) the mean. The highlighted periods represent the model extension.

1st Semester			
	Mean Hs	T mean	Dir Mean
01/01/2007	1.836	7.923	45.616
01/01/2008	1.811	8.079	44.613
01/01/2009	1.894	7.957	44.363
01/01/2010	1.761	8.030	47.253
01/01/2011	1.807	7.982	48.795
01/01/2012	1.767	7.627	52.380
01/01/2013	1.896	8.260	45.486
01/01/2014	1.842	7.758	46.283
01/01/2015	1.810	7.787	46.254
01/01/2016	1.807	7.932	46.986
Mean	1.823	7.934	46.803

2sd Semester			
	Mean Hs	T mean	Dir Mean
01/07/2007	1.642	7.828	72.685
01/07/2008	1.542	7.933	68.535
01/07/2009	1.665	7.779	67.624
01/07/2010	1.628	8.025	70.965
01/07/2011	1.618	7.677	72.726
01/07/2012	1.684	8.098	72.025
01/07/2013	1.625	7.628	71.310
01/07/2014	1.613	7.689	73.940
01/07/2015	1.647	7.549	74.590
01/07/2016	1.591	7.718	70.855
Mean	1.626	7.792	71.526

3.2.1 DELFT3D WAVE and FLOW

FLOW and WAVE modules from DELFT3D were used to translate offshore wave conditions toward near-shore of Pará. DELFT3D is a software that solves the horizontal momentum equations, continuity equations and uses the k-epsilon turbulence closure model. DELFT3D-FLOW is the main hydrodynamics module and can

be coupled with other modules such as WAVE. WAVE module uses SWAN (Simulating WAves Nearshore) and which simulates the propagation and transformation wind-generated waves nearshore DELTARES [44].

The applied hydrodynamic model is averaged over depth (2DH). D3D-FLOW model was online coupled with WAVE. The online coupling is done through the communication file that stores recent flow and wave computations every given time step, in this case, 30 minutes.

The grid was 300 by 250 cells in x and y respectively, with 2700 by 2400 meter resolution (Fig. 3.2). The grid was refined close to the Salinópolis with 1000 by 700 meters resolution.

Pará state has a wide and shallow coastal shelf with the continental shelf break marked by the 100 meter isobath about 200 km away off the coast. ERA Interim results are only valid for deepwater, therefore to guarantee this information for the wave input the model grid is extended 600 km from the coast.

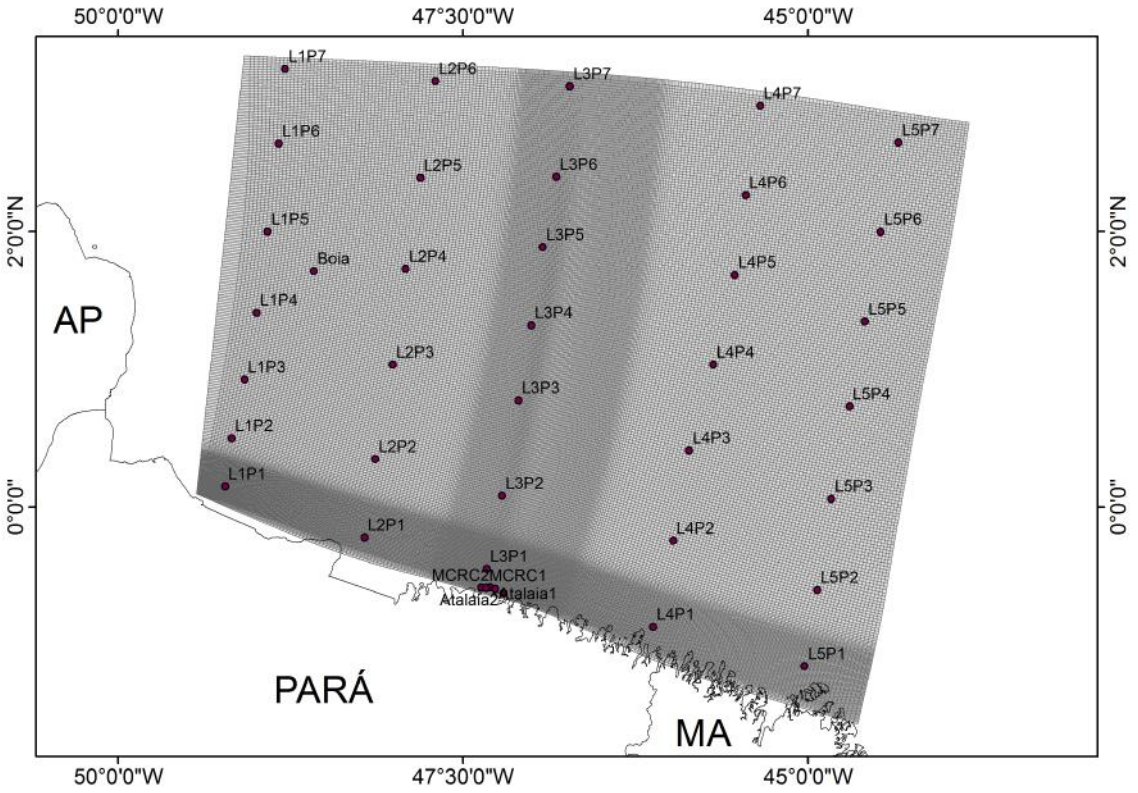

Figure 3.2: Model Grid with 300 by 250 cells. Resolution of 2700 by 2400 meters in x and y respectively. The grid is refined close to Salinópolis with 1000 by 700 meters resolution. The figure also shows the observation points location and their names.

For better stabilization, the initial condition for water level was set to 1 meter as uniform value for the entire domain. Thirty-five observation points were distributed along five parallel lines in deep water and in the AWAC measurements location (Fig.

3.2). In the coastal zone, eleven observation points were set along the beaches (Fig. 3.3).

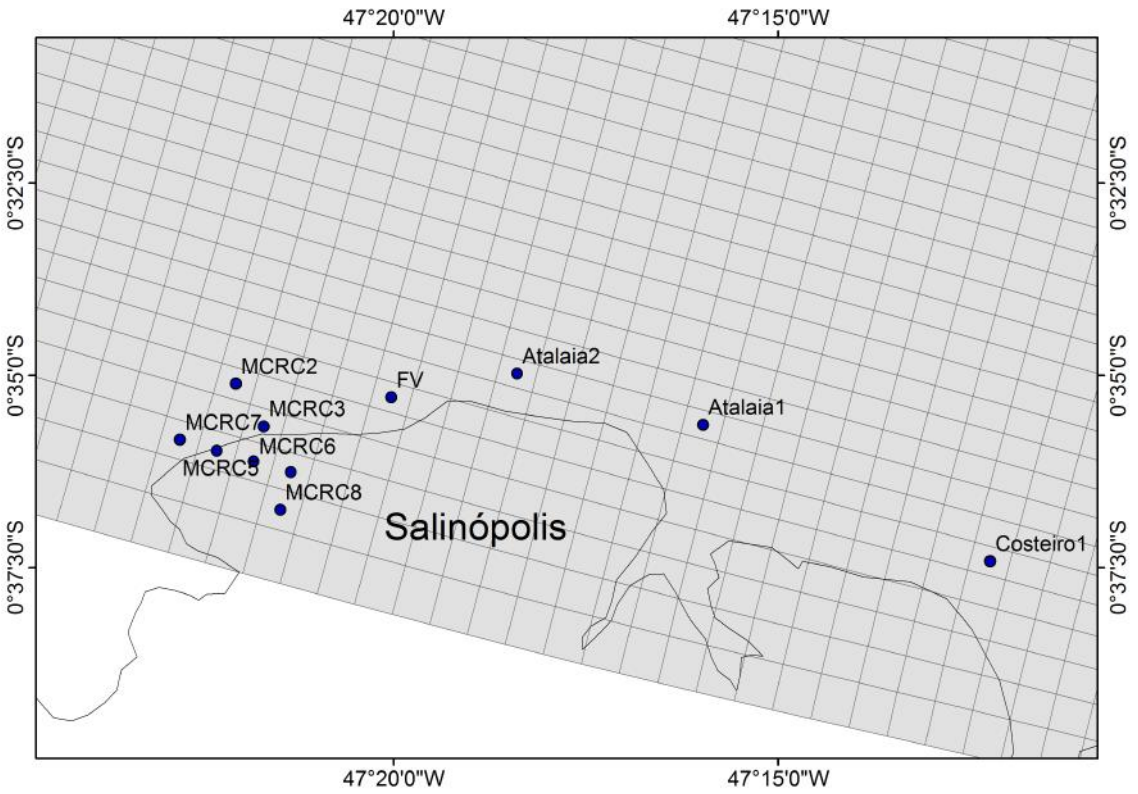

Figure 3.3: Grid Model zoomed at Salinópolis coast with the observation points location and their names. The coastline in the figure is from IBGE database and has lower resolution than the bathymetric data used and thus do not represent the tidal channel between Maçarico and Farol Velho beaches.

The used bathymetric database was obtained from nautical charts published by Brazilian Navy [5]. The charts were: number 21020 (47°40'W 38°05'W; 3°50'S 2°55'N, scale 1:1.000.000) for the east portion of the continental shelf; number 21010 (52°25'W 45°40'W; 1°35'S 8°20'N, scale 1:1.000.000) for the west portion and number 302 (48°07'W 47°10'W; 0°45'S 0°08'N,scale 1:100.000) for refinement close to Salinópolis coast. The result of the bathymetry interpolation used for model runs is presented in figures 3.4 and 3.5. Bottom roughness used a uniform Manning coefficient of 0.0345.

[5] `https://www.marinha.mil.br/chm/dados-do-segnav/cartas-raster`

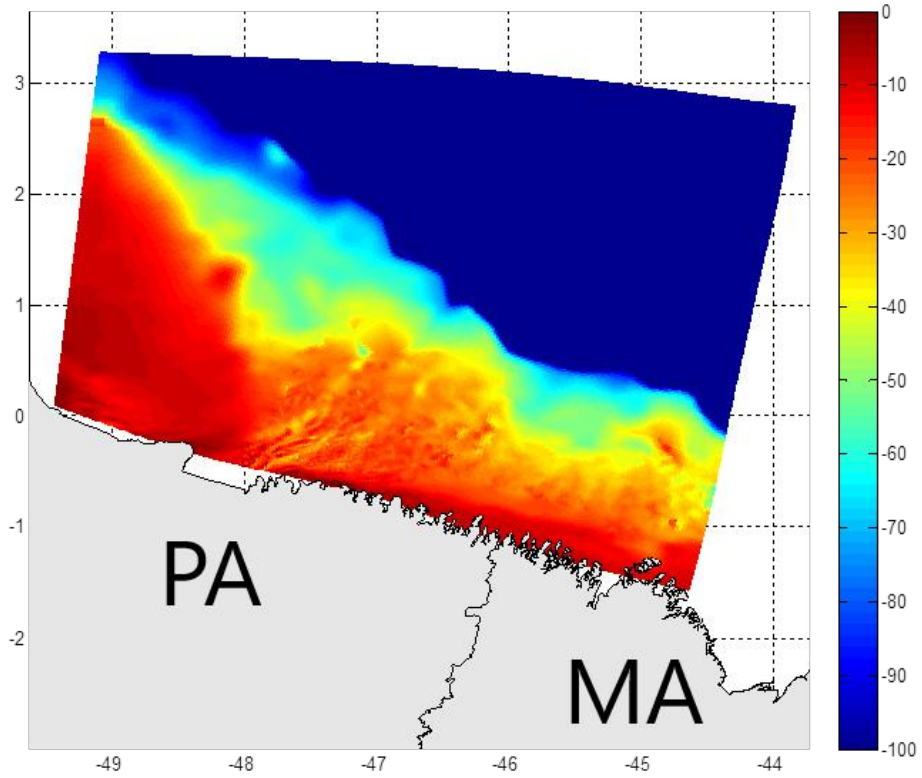

Figure 3.4: Model bathymetry with lower limit set as -100 meter to enhance the continental shelf and the coastal sandbanks.

The hydrodynamic model North boundary condition was defined as harmonic constituents water level from inverse tide model TPXO. TPXO is a global tide model that uses the least square fit of the Laplace Tidal Equations and the along track averaged data from TOPEX/Poseidon and Jason [45]. East and West boundaries were set with Neumann conditions as zero gradient. Neuman condition calculates the gradients inside the model, reproducing it in the boundaries leading to a more stable flow inside the domain.

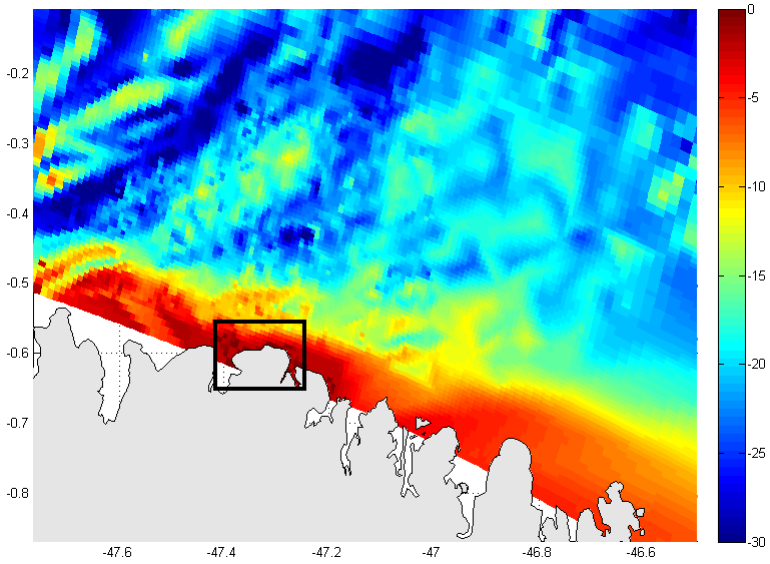

Figure 3.5: Detail of model bathymetry at Salinópolis coast with lower limit set as -30 meters to enhance the coastal sandbanks.

The wave model North and East boundaries conditions were set with wave parameters significant wave height (Hs), peak period (Tp) and wave direction from ERA-Interim 6-hourly output. Wave parameters from ERA-Interim showed low spatial variation in deep water close to Salinópolis (3°N, 45°to 48°W): lower than 20 cm in wave height, up to 5° in wave direction and less than 1 second in wave period. Therefore, a time-varying series at a single point near northeast model grid corner (3° N, 46.5° W) were used as input for both boundaries.

3.2.2 Data Available for Model Comparison

Water level data from Brazilian Navy station were used to get astronomical constituents for the coast with python package Pytides [6]. Salinópolis anchorage station data were retrieved from Brazilian Navy Database (Banco Nacional de Dados Oceanográficos - BNDO [7]). The dataset is about one year long from 1 January 1955 to 30 December 1955. According to the Navy information, the station is located at 0°37'0" S and 47°21'0" W. However, these coordinates correspond to a location on land near the municipal center of Salinópolis (Fig. 3.1). Hence, the real location of measurement is unknown. Coastal water level model output was compared with the tidal prediction from Salinópolis anchorage.

For wave model validation we used an Acoustic Wave and Current profiler (AWAC) data. AWAC measurements consisted of 12 campaigns, lasting up to 48

[6] `https://pypi.python.org/pypi/pytides/0.0.4`
[7] `https://www.marinha.mil.br/chm/chm/dados-do-bndo/bndo`

hours each, from June 2011 to May 2012 (Tab. 3.4). Located at 1,7° N 48.58° W (represented by the point named 'boia' in fig. 3.2) in a water depth of 20 m, the equipment was set to measure 34 minutes of wave data at 1Hz every hour. AWAC also registered a 600 seconds current ensemble and one water level value per hour. Direction measurements from AWAC were compensated from the magnetic declination of 19°30'W [24]. The period from 1 June 2011 to 31 August 2011 was used to validate model results along with AWAC data. This corresponds to the second and third campaigns (Tab. 3.4) chosen due to its longest record (48 and 26 hours respectively).

Table 3.4: Duration and the tidal regime of the two campaigns used for model validation. Measurements of wave and currents were made with an AWAC in a water depth of 20 meters near the Amapá coast. The exact location of the measurement is represented in figure 3.2 by the point named 'boia'. Date format is day/month/year.

Duration (hours)	Date	Tide
16	09/06/2011 - 14/06/2011	Neap tide
48	29/07/2011 - 04/08/2011	Spring tide

The Root-Mean-Square-Error (RMSE) and the bias were calculated for model validation. The RMSE (Eq. 3.1)represents the standard deviation of the differences between predicted and observed values (residuals). It is a measure of how spread out these residuals are from a regression line.

$$RMSE = \sqrt[2]{\frac{1}{N}\sum_{i=1}^{N}(X_m - X_o)^2} \tag{3.1}$$

In equation 3.1, N is the time-series length, X_m indicates the model data point and X_o represents observation data point. The unbiased Root Mean Square Error (uRMSE) were also calculated (Eq. 3.2). It indicates the variability of the model relative to the data. uRMSE is zero when model result and observed data have equal variability.

$$uRMSE = \sqrt[2]{\frac{1}{N}\sum_{i=1}^{N}[(X_{mi} - \overline{X_m}) - (X_{oi} - \overline{X_o})]^2} \tag{3.2}$$

In equation 3.2 the $\overline{X_m}$ and $\overline{X_o}$ represent the mean value over model and observation data, respectively. The bias (Eq. 3.3) indicates how model over- or underestimates observation measurements.

$$bias = \overline{X_m} - \overline{X_o} \tag{3.3}$$

Some issues faced during the process concerning bathymetric data and the lack of measurements in the region were presented. The extension of the modeled area forced the use of three nautical charts that overlap with a different value at the same point. Brazilian North coast is a dynamic area with migrating sandbanks, an additional difficulty for measurements. This characteristic results in a lack of collected data for the region. Few data that exist either have imprecise information, like the wrong location of the tide gauge or represents a short period series (longer AWAC measurements are only 48 hours long).

3.2.3 Model and Data Comparison

Results from wave model in the same location of the AWAC measurements (1,7° N 48.58° W) were compared. Two periods were used for comparison: 48 hours record from 31 July 2011 to 2 August 2011 and 26 hours record from 27 August 2011 to 28 August 2011. The model well reproduces the data.

Statistics for the first period (31 July 2011 to 2 August 2011) shows that model overestimated wave height in 10 centimeters and underestimated wave period in 0.66 seconds (Tab. 3.5). Considering the absolute value of RMSE we might conclude that the distribution of residuals from wave direction is more spread out than the wave height and period. However, the relative value is insignificant since we must consider the total range for each variable: a spread of 5° from a total of 360° correspond to only 1.39%.

Table 3.5: (Unbiased)Root Mean Square Error and Bias from model and data comparison for the period between 31 July 2011 and 2 August 2011

	Hs	Tp	Direction
RMSE	0.1394	1.0398	11.635
uRMSE	-0.0887	-0.8028	5.2213
Bias	0.1079	-0.6617	10.3900

Modeled peak period (Fig. 3.6) varied significantly less than the measured peak period and wave direction was biased in 10°. The unbiased RMSE of wave height and peak period close to zero shows that the model follows data variability. Direction uRMSE is higher indicating that model did not follow variability of the measurement although figure 3.6 shows some similarity. This could be due to a time lag between model and data. Significant wave height and peak period comparison between the model and the data are in figure 3.6.

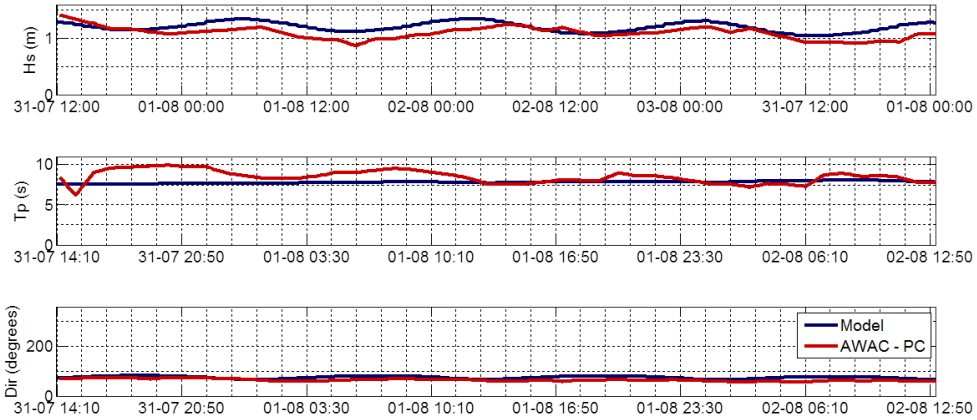

Figure 3.6: Significant wave height (top); Wave peak period (middle) and Wave direction (bottom) comparison between the model (blue line) and the AWAC data (red) for the period from 31 July to 2 August 2011.

In the second period (27 August 2011 and 28 August 2011) model results underestimated wave height in 15 centimeters and underestimated wave period in 0.22 seconds (Tab. 3.6). Figure 3.7 shows the comparison between measured and modeled significant wave height, peak period and wave direction from model results and AWAC measurement. Modeled wave direction was biased in -2.74°. The uRMSE was twice higher than the previous period (-1.69 vs -0.8, respectively). Direction uRMSE were a little lower than the previous result (4.34 vs 5.22). RMSE shows that the distribution of the residuals of the wave direction is more spread out than the wave height and period. Modeled peak period (Fig. 3.7) varies significant less than the measured peak period.

Table 3.6: Statistics of model and data comparison for the period between 27 August 2011 and 28 August 2011

	Hs	Tp	Direction
RMSE	0.1770	1.7088	5.1563
uRMSE	-0.0916	-1.6950	4.3463
Bias	-0.1517	0.2170	-2.7414

Graphical results show a good agreement between the model and the measured data, though those are very short periods to consider (24 and 48hrs) especially for statistics. This could explain why statistics from the two periods differ. Also, there is a phase lag between the timeseries but it is not consistent. For example, wave height peak is almost 90° out of phase at 19:00 of 2 August 2011 (Fig. 3.6), with the model in advance, while it seems to agree well with the rest of the time series.

On the second period comparison, at figure 3.7, modeled wave height is delayed in relation to AWAC measurements.

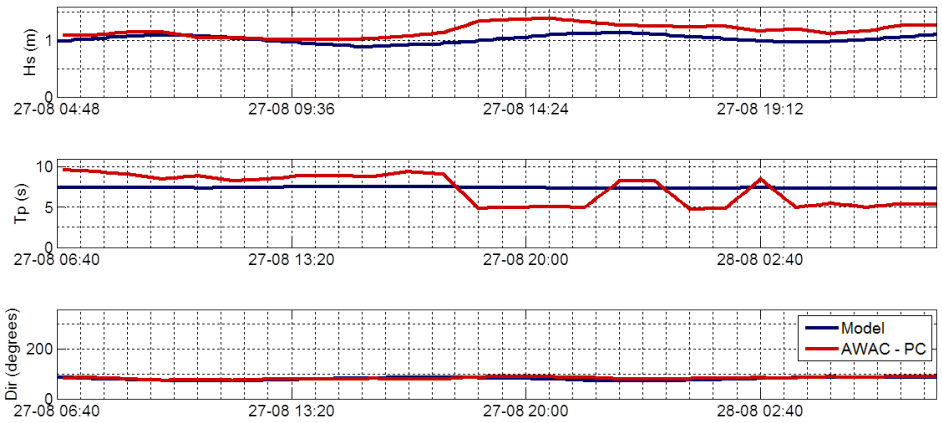

Figure 3.7: Significant wave height (top); Wave peak period (middle) and Wave direction (bottom) comparison between the model (blue line) and the AWAC data (red) for the period from 27 August 2011 to 28 August 2011.

Peak period variation was the only parameter with no agreement between data and model. However, both are in the same order of magnitude. Differences between them might be caused by a high-frequency signal not captured by the model or not represented by the input data. ERA-INTERIM outputs were used as input with a time step of 6 hours.

3.2.4 Sediment Transport

Wave model results were used for an analytical analysis of the sediment transport capacity using the formulation proposed by WALTON e DEAN [46]. Significant wave height and wave direction at a point close to Maçarico beach (point MCRC2 in fig. 3.3) at a water depth of 5 meters, located approximately 2000 meters away from the coast of Maçarico, was used for the calculations. For each wave direction, the significant wave height was calculated using a weighted average. The shoreline angle of Maçarico and Corvina beaches range from -15° to 75° with a 5° step.

$$Q_l = \frac{k H_b^{\frac{5}{2}} \sqrt{\frac{g}{\lambda}}}{16(\frac{\rho_s}{\rho_w}(1-p))} \sin 2(\beta - \alpha_b) \tag{3.4}$$

In this equation, α is the wave direction at the breaking point, β is the shoreline angle given by the angle of a perpendicular line, H_b is the wave height at the breaking point. Water density ρ_w was set as 1025 $Kg.m^{-3}$ and sediment density ρ_s were set as 2650 $Kg.m^{-3}$ according to CEM [47] for sand. The empirical calibration coefficient (k) varies from 0.4 to 1 and must be estimated with field observation. In the absence

of data measurement, the coefficient was set to its neutral value. λ is the ratio of wave breaking height to water depth and is set as 0.78.

Q_l is the longshore transport capacity expressed in $m^3.yr^{-1}$. There are two possible directions of motion, toward the right or to the left, relative to an observer standing on the shore looking out to the sea. As a standard convention, drift moving to the left (right) are negative (positive) [46]. Results of this equation are presented as a littoral drift rose (LDR), a polar graph representation where the transport rate varies with the beach orientation having the same wave climate [46]. LDR graph presents positive and negative drift as well as the net drift - the sum of the positive and negative values - and the gross drift - the sum of the absolute values of the positive and negative transport.

Chapter 4

Physical Characterization

4.1 Wind

The Equatorial zone is under influence of Intertropical Convergence Zone (ITCZ) with seasonal variation in wind direction and intensity [20]. Figure 4.1 shows intensity variation based on INMET data with an increase in wind speed during the second semester of the year. The highest mean wind speed is observed in September (approx. 4 $m.s^{-1}$) and the lowest in April (approx. 1.7 $m.s^{-1}$). Wind speed can reach values great than 6 $m.s^{-1}$ all over the year (Fig. 4.1).

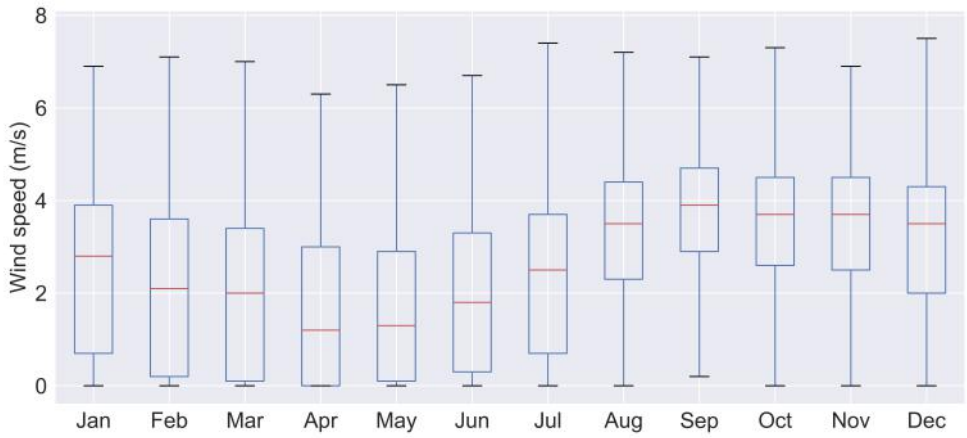

Figure 4.1: Box plots of wind speed throughout the year. The box extends from the lower to upper quartile values of the data, with a red line at the median. The whiskers extend from the box to show the range of the data. The months of the years are distributed on the X-axis and Y-axis is the wind intensity in $m.s^{-1}$

Wind from East and Northeast are predominant throughout the year (Fig. 4.2). An increase in the occurrence of East wind from June to September is associated with the most Northward position of ITCZ [20]. East and Northeast are the directions with the strongest wind intensity.

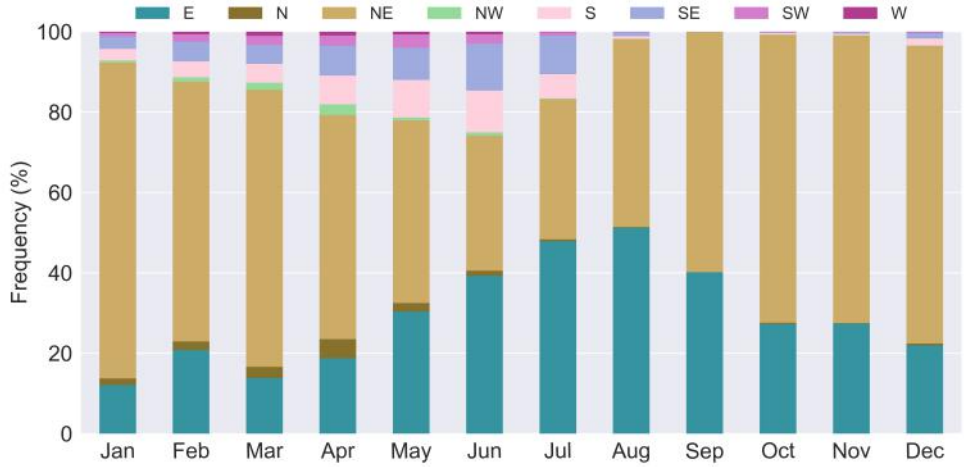

Figure 4.2: Frequency distribution of wind direction by months. Each column in X-axis represents a month and the Y-axis the frequency of occurrence. Each color represents one of the eight main wind direction: East (blue), North (brown), Northeast (dark yellow), Northwest (light green), South (light pink), Southeast (light purple), Southwest (pink), West (purple).

On a daily scale, wind speeds are higher between 8 AM and 5 PM (Fig. 4.3). During daytime, an increase of the frequency of East and North winds occur. Early in the morning and night hours, the frequency of South and Southeast winds increases (Fig. 4.4).

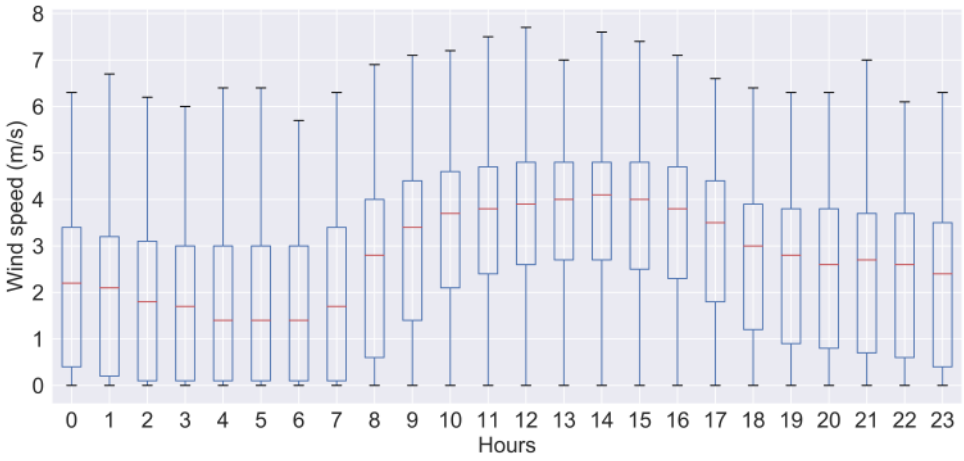

Figure 4.3: Box plots of wind intensity by hours. The box extends from the lower to upper quartile values of the data, with a line at the median. The whiskers extend from the box to show the range of the data. Day hours are distributed on the X-axis and Y-axis is the wind intensity in $m.s^{-1}$

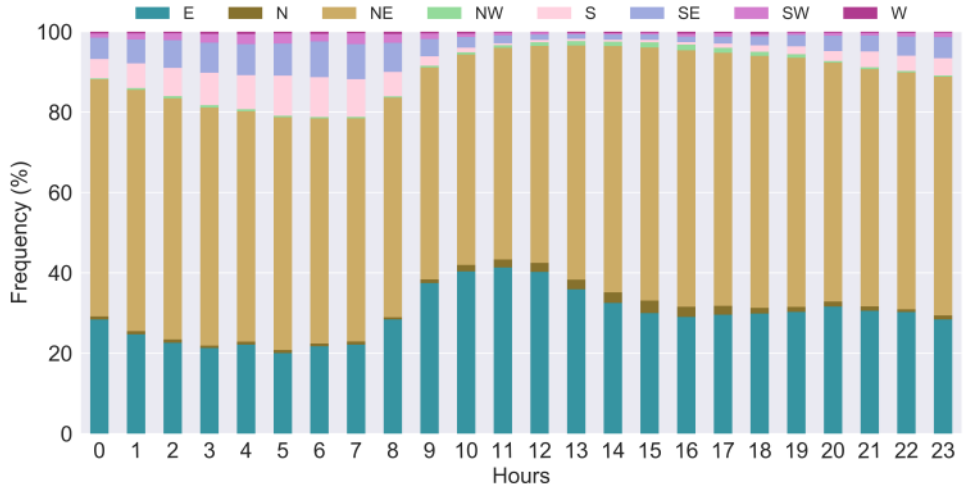

Figure 4.4: Frequency distribution of wind direction along day hours. Each column in X-axis represents an hour and the Y-axis the frequency of occurrence. Each color represents one of the eight main wind direction: East (blue), North (brown), Northeast (dark yellow), Northwest (light green), South (light pink), Southeast (light purple), Southwest (pink), West (purple). An increase in the frequency of East and North directions between 8 AM and 5 PM and South and Southeast during the night and early morning.

4.2 Rainfall

In this study, we will apply a more specific division than the one on section 2.1. January to May compose the wet season and August to November the dry season, and we included a transitional period on June, July and December (Fig. 4.5). This division considers the rainfall volume and the touristic activities that already occurs in the city.

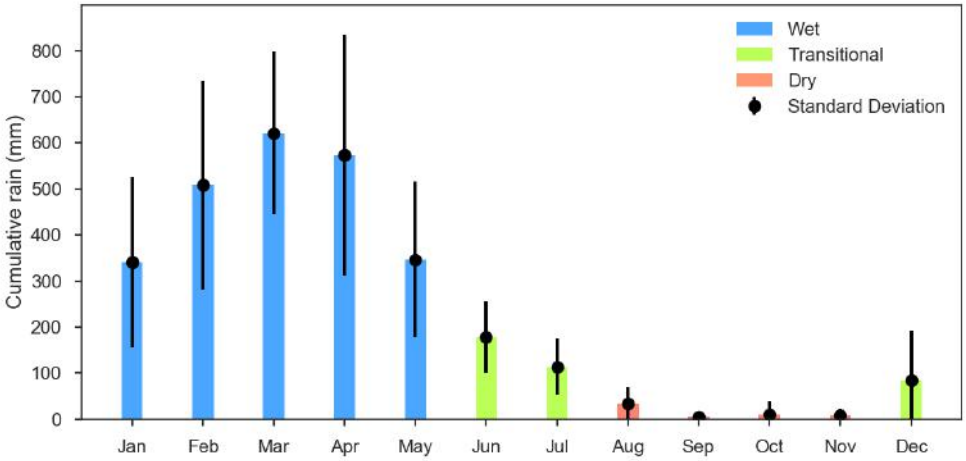

Figure 4.5: Precipitation climatology from thirty-seven years data from Brazilian National Water Agency (ANA). Data range from 1 January 1978 to 31 December 2015.

Table 4.1 shows the difference in rain volume between wet, transitional and dry months. The volume of rainfall in the wet months varies from 621.02 mm to 1375.3 mm. The transitional period varies from 84.11 mm to 178.73 mm. During the dry season mean values range from 5.36 mm to 34.84 mm.

Table 4.1: Precipitation mean per month and season, with minimum and maximum values in $mm.month^{-1}$. The table is divided into wet (blue shaded), transitional (green shaded) and dry (orange shaded) seasons.

	Month Mean (mm)	Mean (mm)	Max (mm)	Min (mm)
Jan	341.22	478.01	1375.3	23.3
Feb	507.85			
Mar	621.02			
Apr	573.18			
May	346.81			
Jun	178.73	125.65	569.29	2.4
Jul	114.11			
Dec	84.11			
Aug	34.88	14.83	182	0
Sep	5.36			
Oct	10.56			
Nov	8.54			

February to April is the period with higher mean rainfall volume, ranging from 507.85 mm to 621.02 mm in one month. Those values correspond to almost half of the annual rainfall volume in the state of Rio de Janeiro (1345 $mm.yr^{-1}$) and São Paulo (1576 $mm.yr^{-1}$) [1]. The mean rainfall volume for the wet season is 478 $mm.month^{-1}$, more than three times the mean rainfall volume in the transitional season and an order of magnitude greater than the dry season.

March is the wettest month with an average of 26 days rainy days (also the highest in terms of volume of rain with 621.02 mm). March also has on average 16 consecutive rainy days, reaching 22 days in wet years and 10 days in dry ones. In contrast, dry season months have on average less than 5 days of rain per month and less than 40 mm of total rain volume (Fig. 4.6). Among the transitional months (June, July and December), June is the wettest month with an average of almost 180 mm and 15 rainy days. These values are considerably lower than those observed during the wet months, supporting the proposed seasonal division.

[1] http://www.inmet.gov.br/portal/index.php?r=clima/normaisClimatologicas

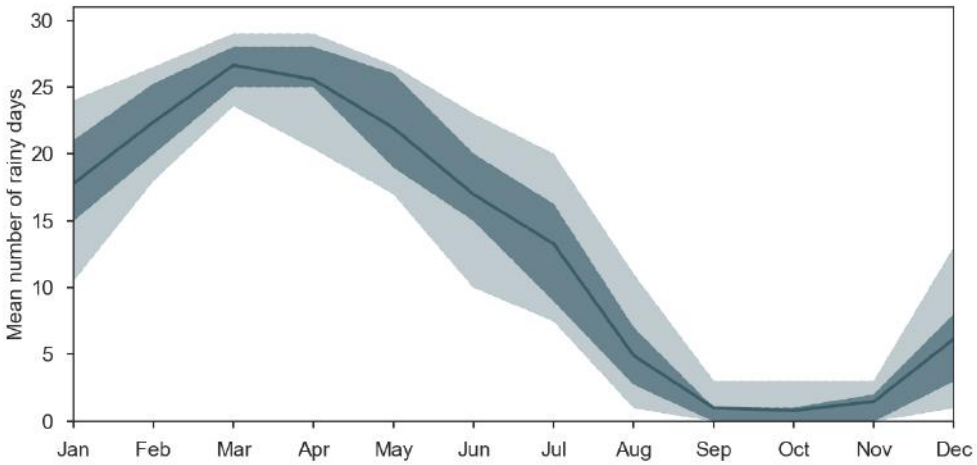

Figure 4.6: Month distribution of an average of rainy days (rain volume higher than 0.2 mm). The blue line represents the mean number of rainy days over the months with 25th to 75th (dark shadow) and 10th to 90th (light shadow) percentile bands. Line peaks in March when 26 out of the 31 days of the month register rainfall.

Rain is well distributed over the day during the wet season, with a maximum mean value at 4:00 AM (Fig. 4.7). Those values are estimated by the simple mean of all register per hour, being sensitive to extreme registers. Two registers in 2016 were responsible by the elevation of the 4:00 AM mean: the occurrence of 30 mm of rain on 29 March 2016 and 35mm in 03 April 2016. The probability of rain occurrence (values higher than 0.2 mm) along the day is only 0.48% on dry months, 4.8% during transition season and 13.84% during the wet season. Nevertheless, it is not possible to determine a well-defined rain pattern along the day as in the capital, Belém - known by the 4:00 PM rain.

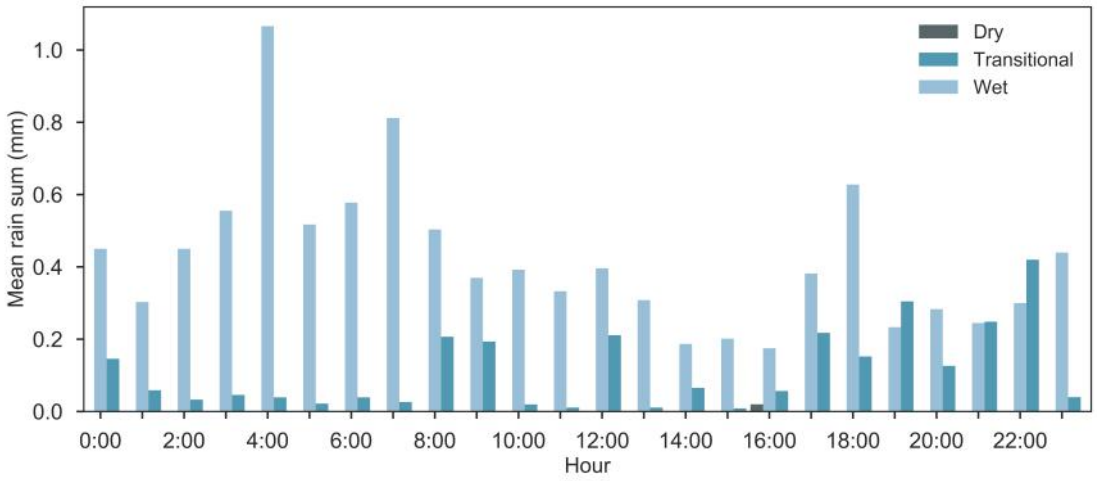

Figure 4.7: Distribution of the mean volume of rain per hour in wet (true blue), dry (dark blue) and transitional (light blue) seasons. A minimum value of 0.2 mm was set to consider only days with rain register and disregarding zero values.

Considering values from figure 4.7 and the classification of rain intensity from the International Civil Aviation Organization (ICAO) (Tab. 4.2) [2], precipitation during the wet season is classified as moderate drizzle to heavy drizzle while during the transitional months would be classified as moderate drizzle, with a maximum mean of 0.4 $mm.hr^{-1}$ at 10 PM. Using the limit value between rain and drizzle (2.5 mm) on table 4.2, the probability of drizzle occurrence is 0.32%, 3.26% and 9.70% during dry, transition and wet season respectively. The probability of having rain volumes higher than 2.5 mm, follows the same pattern, 0.16%, 1.54% and is 4.13%. Disregarding values lower than 2.5 mm, the rain volume average for wet and transitional months is about 7 $mm.hr^{-1}$ and is classified as moderate rain. There is a chance of 0.07%, 0.74% and 2.01% of having the occurrence of a rain volume higher than 5 $mm.hr^{-1}$ (heavy rain) in dry, transition and wet season respectively.

Table 4.2: Precipitation intensity classes according to the International Civil Aviation Organization (ICAO).

	Light	Moderate	Heavy
Drizzle	$< 0.1\ mm.hr^{-1}$	0.1 to 0.5 $mm.hr^{-1}$	$> 0.5\ mm.hr^{-1}$
Rain	$< 2.5\ mm.hr^{-1}$	2.5 to 10.0 $mm.hr^{-1}$	$> 10.0\ mm.hr^{-1}$

4.3 Water Level and Tidal Currents

Figure 4.8 shows tidal prediction for Salinópolis anchorage from 1 December 2010 to 31 January 2011. Salinópolis tidal regime is semidiurnal with a tidal range of 2 meters during neap tide and 4 meters during spring tide. This characterizes a macrotidal regime.

Water level at Salinópolis varies 3 to 4 meters in 6 hours. Rapid water level variation is responsible for strong currents specially at confined regions like channels and estuaries.

Figure 4.9 shows currents magnitude and direction in the tidal channel between Maçarico and Farol Velho for the first measurement period. On the top of figure 4.9 pressure level along the measurement period evidences the exposure period, when water level was null. Measurements were filtered in order to exclude those registers. Currents flow in a main direction East - West according to the channel orientation and ebb currents (0.4 $m.s^{-1}$) were more intense than flood currents (0.2 $m.s^{-1}$).

[2] https://www.icao.int/safety/meteorology/amofsg/AMOFSG%2016%20Archive%20Material/AMOSSG%206/SNs/AMOSSG.6.SN.010.5.en.doc

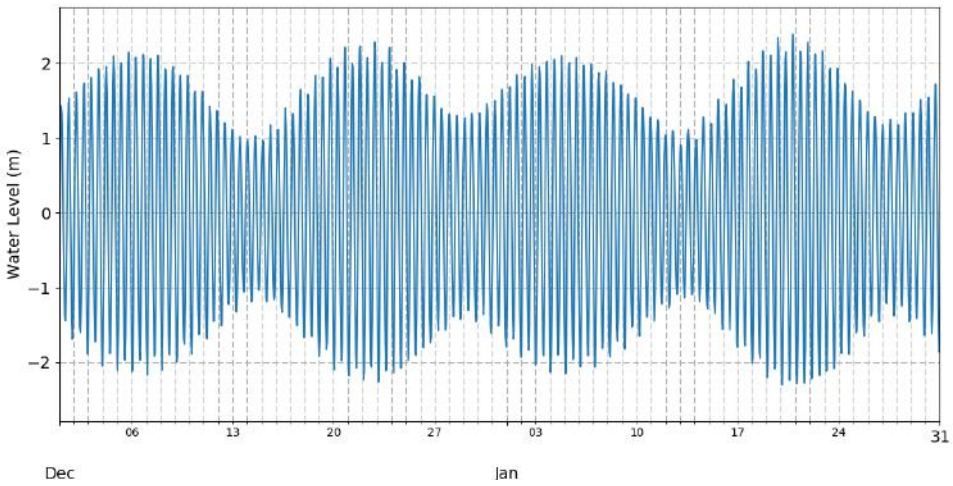

Figure 4.8: Tidal prediction for Salinópolis Anchorage from 1 December 2010 to 31 January 2011. Y-axis shows water level in meters.

During the second measurement period (Fig. 4.10), flood reached 0.5 $m.s^{-1}$ while ebb were about 0.3 $m.s^{-1}$. Some differences about the acquisition might be the cause of those results: the first period was only 24 hours long and recorded during two tidal cycle. Water level at high tide were 2.1 meters and 2.4 meters. The second time series was about 53 hours long, with four tidal cycles. Water level at high tide were higher (1.5 m; 1.7 m; 2.5 m; and 3.0 m) at this period, including part of spring tide.

Strong tidal currents as shown could be a potential risk for swimmers and beach-goers. Tidal currents would also play an important role in sediment transport. An specific campaign would be necessary for a better understanding of the tidal channel behavior, thus those are preliminary results of the available measurements.

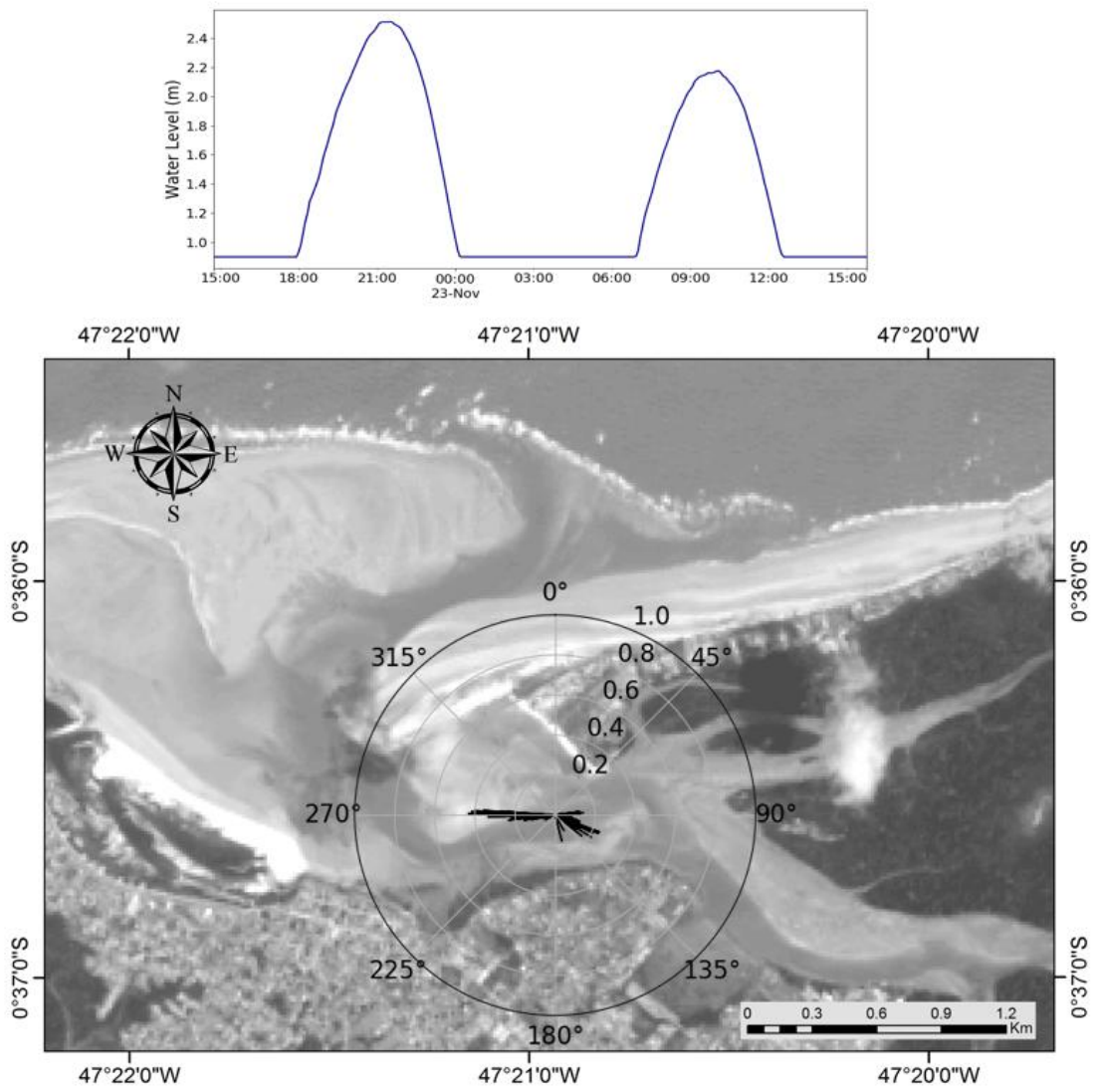

Figure 4.9: ADV measured for 24 hours starting on 22 November 2017 at 15:00. Pressure level from ADV sensor (top) during current measurement in the tidal channel. Y-axis shows water level in meters and X-axis is the date and hour of measurement. On the map, the current polar graph with intensity in meters per second and direction is toward.

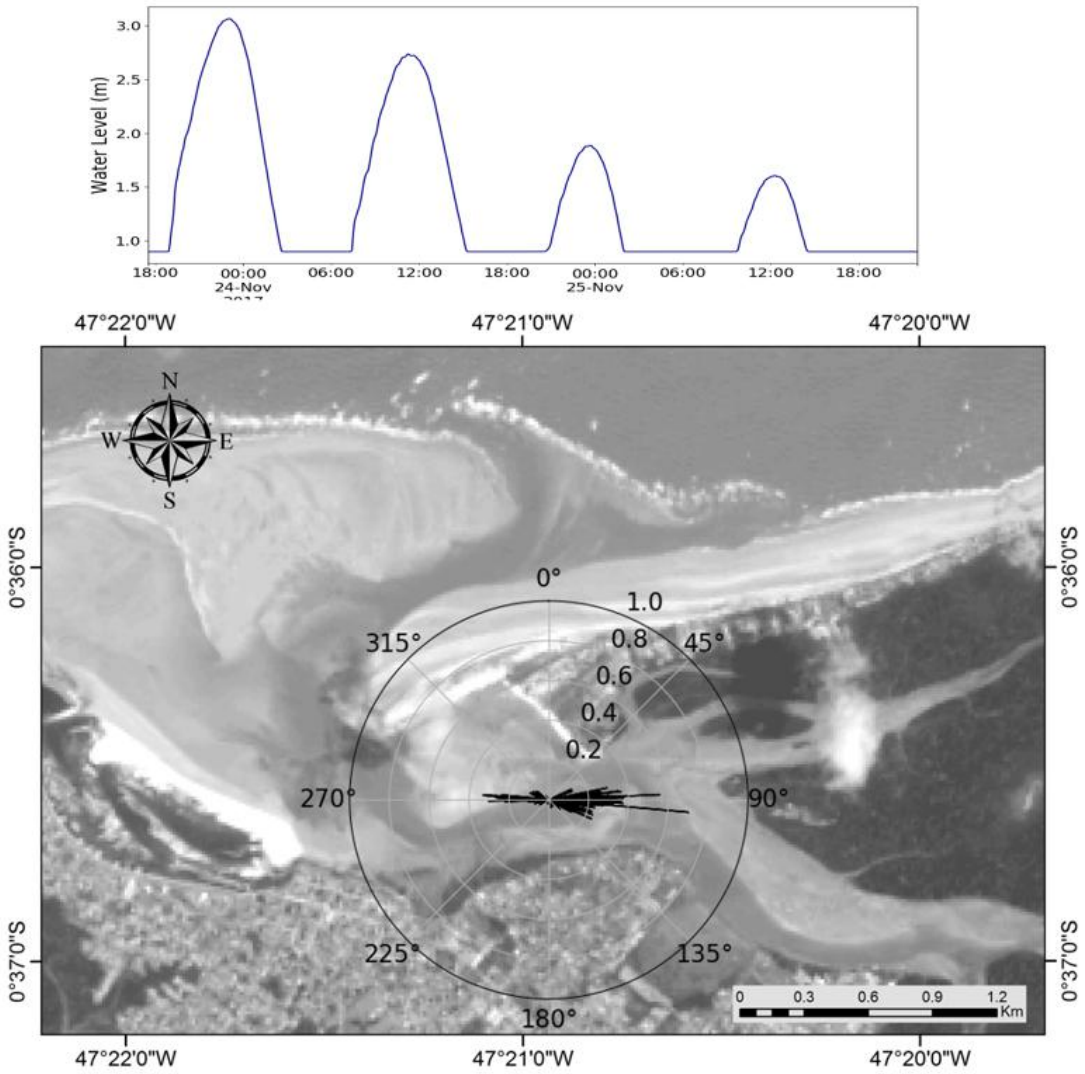

Figure 4.10: ADV measured for 48 hours starting on 23 November 2017 at 18:00. Pressure level from ADV sensor (top) during current measurement in the tidal channel. Y-axis shows water level in meters and X-axys is the date and hour of measurement. On the map, the current polar graph with intensity in meters per second and direction is toward.

4.4 Waves

The continental shelf in front of Salinas is wide and shallow, therefore waves lose energy as they propagate towards the coast due to bottom friction and wave breaking on sandbanks as well as they have enough time to refract. The wave modification leads to small seasonal variation at the coast when compared to deep water where Hs varies from 1 meter in lower wave season to 3 meters in high wave season.

The model result at point L3P1 (close to Salinópolis, at a water depth of 24.5 m) shows a seasonal variation of wave height with lower Hs (0.6 m) from June to

October and an increase (reaching 1.15 meter) from November to April (Fig. 4.11). At the observation point MCRC2 (at 4 meters depth on Maçarico beach), wave height was lower than at point L3P1 with a maximum value of less than 0.5 m from June to October and waves of 0.8 m in January (Fig. 4.12).

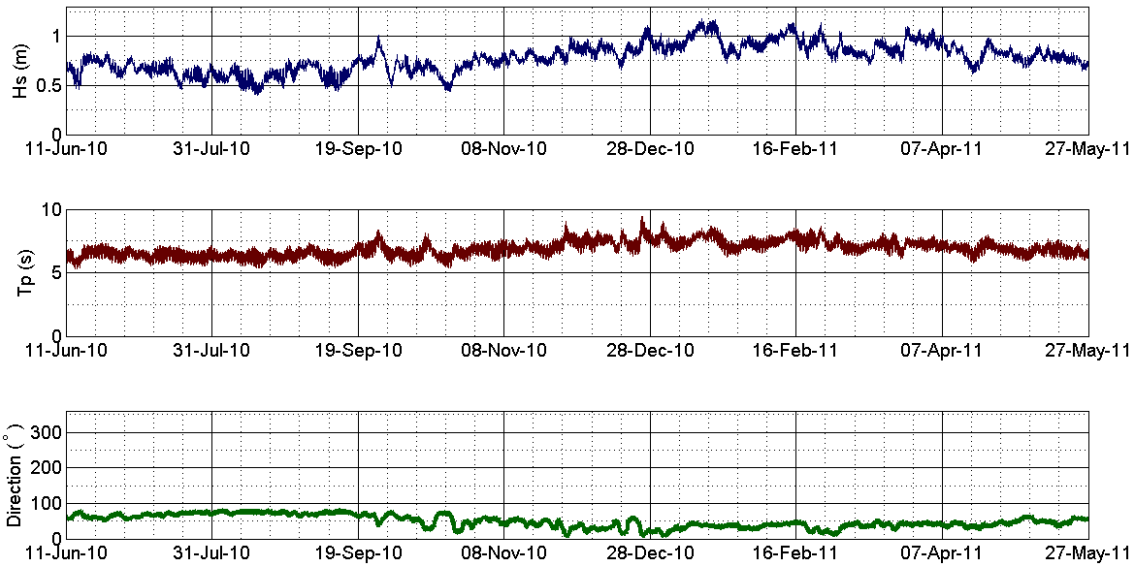

Figure 4.11: Model result of wave height (blue line on the top graph), peak period (red line in the middle) and wave direction (green line in the bottom graph) at observation point L3P1 at 24.5 meters depth

The model result agrees with *in situ* observations at Corvina beach from RANIERI [28] (0.44 to 0.63 m in April and 0.60 to 0.65 m in October) and PEREIRA *et al.* [31] (1.1 to 1.5 m in March and 1 to 1.2 m in September and October).

Figure 4.11 shows variation of about 50° in wave direction (80° on the first semester and 30° on the second semester). It has a negative correlation with wave height (higher(lower) waves with lower(higher) wave direction). At MCRC2 point (Fig. 4.12) wave diffracted due to shallow water and wave direction has less significant variation throughout the year - from 40° from June to October to 20° from November to May. Peak period at the coast varies from 7 to 9 seconds and a positive relation between wave height and peak period could be observed both on figure 4.11 and figure 4.12.

Model simulation captured the wave energy dissipation due to sandbanks. Time-series from points along the third line (L3) shows wave height decreasing as we approach the shore (Fig. 4.13). Figure 4.13 shows a difference of almost 0.5 meters from wave height from point L3P3 (at a water depth of 39 m) to point L3P1 (at 24 m depth) and from L3P1 to MCRC2 (at 4 m). Wave losses energy in its way to the coast due to bottom friction and wave break on sand banks.

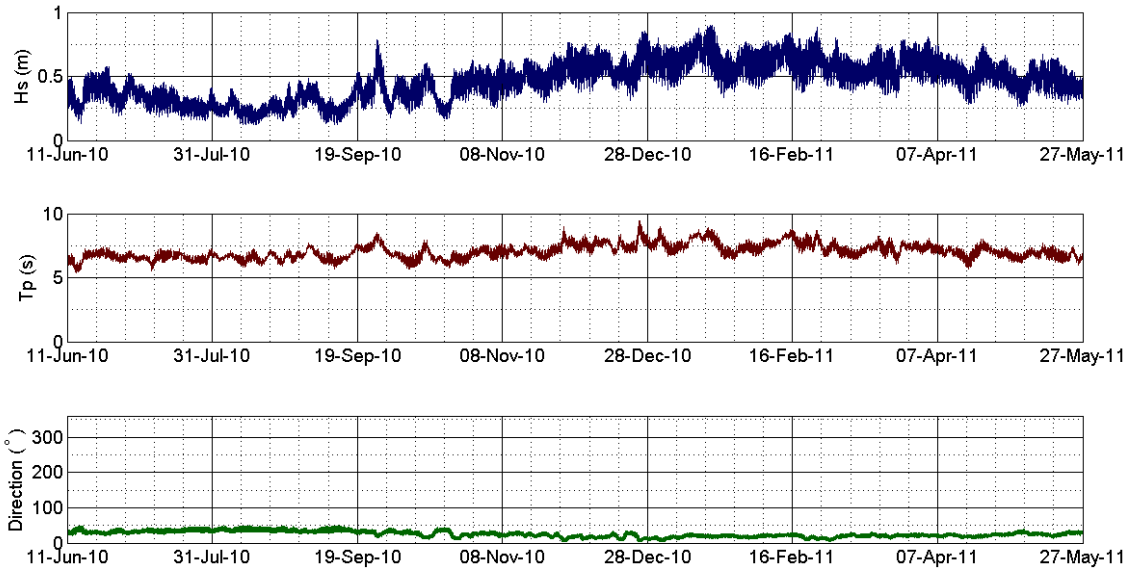

Figure 4.12: Model result of wave height (blue line on the top graph), peak period (red line in the middle) and wave direction (green line in the bottom graph) at observation point MCRC2 at 4 meters depth

Tidal modulation of wave height and period, described in section 2.3, were represented in the model simulation by the coast (Fig. 4.14). In figure 4.14, tidal amplitude (black solid lines) affects wave height (red dashed line) and period (blue dashed line). With the increase of water level, higher waves with greater peak period reach the coast. During low tide sandbanks dissipate wave energy and only lower waves with short crest are observed.

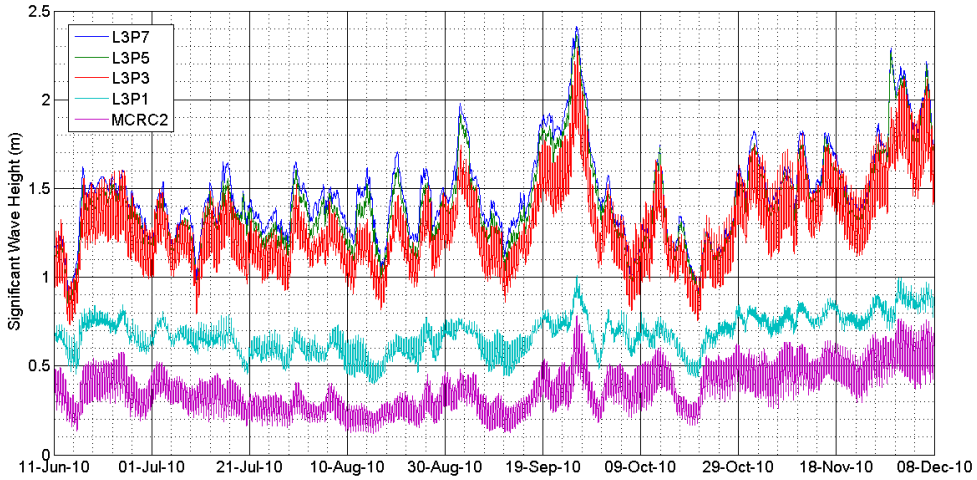

Figure 4.13: Wave height attenuation effect due to submerged sandbanks could be observed in model result. Water depth decreases in the order: L3P7 (2731 m); L3P5 (547 m); L3P3 (39 m); L3P1 (24 m); MCRC2 (3.7 m).

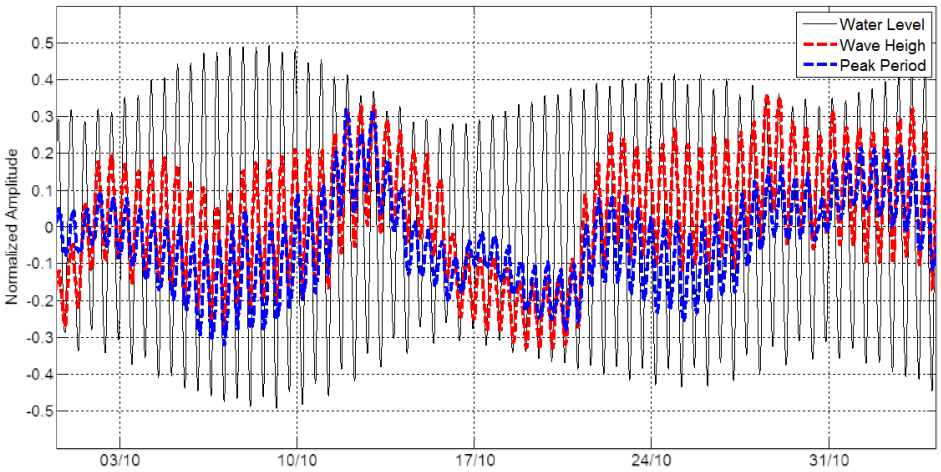

Figure 4.14: Tidal modulation of wave height and period could also be observed in the model result. Water depth (solid black line), wave height (dashed red line) and peak period (dashed blue line) were normalized for a better graphical presentation.

Wave climate based on model results at the point L3P1 (24 meters) and MCRC2 (4 meters at Maçarico beach) are shown in figures 4.15 and 4.16. Wave climate at L3P1 (Fig. 4.15) seasonally changes in terms of direction and intensity. The prior wave direction from November to April is Northeast with wave height from 0.76 m to 1.2 m. From June to October, major wave direction is from East-Northeast with wave height from 0.54 m to 0.87 m.

By the coast, wave climate is more uniform in terms of wave direction (Fig. 4.16). Waves from North-Northeast is predominant throughout the year. From June to October, waves from Northeast also occurs. Wave height is higher from November to April (0.43 m to 0.87 m) than from June to October (0.21 m to 0.65 m).

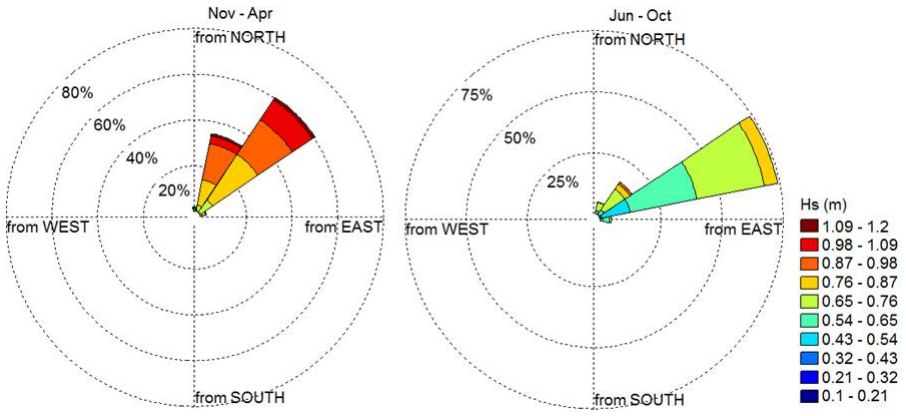

Figure 4.15: Wave rose from the model result at point L3P1. Waves come from the indicated direction and colors represents significant wave height (Hs) in meters.

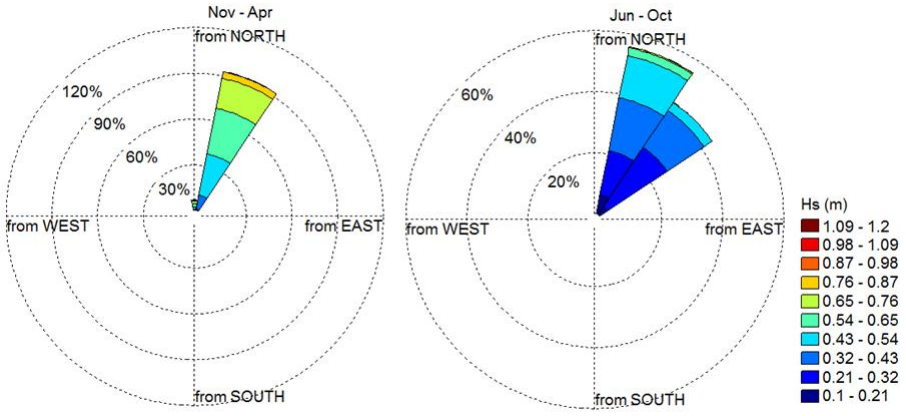

Figure 4.16: Wave rose from the model result at point MCRC2. Waves come from the indicated direction and colors represents significant wave height (Hs) in meters.

4.5 Sediment Transport Analysis

Wave climate at MCRC2 point were used to estimate sediment transport on Maçarico and Corvina beaches. An annual analysis were made. WALTON e DEAN [46] formulation considers changes in wave direction, thus is not necessary to divide sediment transport into seasons.

Figure 4.17 shows transport values per beach orientation in millions cubic meters per year ($10^6\ m^3.yr^{-1}$). This type of chart fixes the beach angle and represents the sum of positive or negative transport values according to wave attack angle. Negative (positive) values represent transport toward left (right) relative to an observer standing on the shore and looking out to the sea.

The left polar graph on figure 4.17 shows positive (blue) and negative (red) values of transport for beach orientation from 345° to 75°. This beach orientation represents Maçarico and Corvina shoreline orientation. The graph shows a change in the direction of the sediment transport for a beach orientation of 40° which is the prior wave attack angle.

The right graph on figure 4.17 represents the difference between positive and negative transport, the net transport, for each beach orientation. The lowest net transport is in 20° (945 $m^3.yr^{-1}$) and the highest are at 65° (14900 $m^3.yr^{-1}$) and 345° (14800 $m^3.yr^{-1}$). Figure 4.18 shows the total transport disregarding its direction and the lowest value is at 20°. Sediment transport values might be significant higher due to the tidal currents influence, not considered in the calculations.

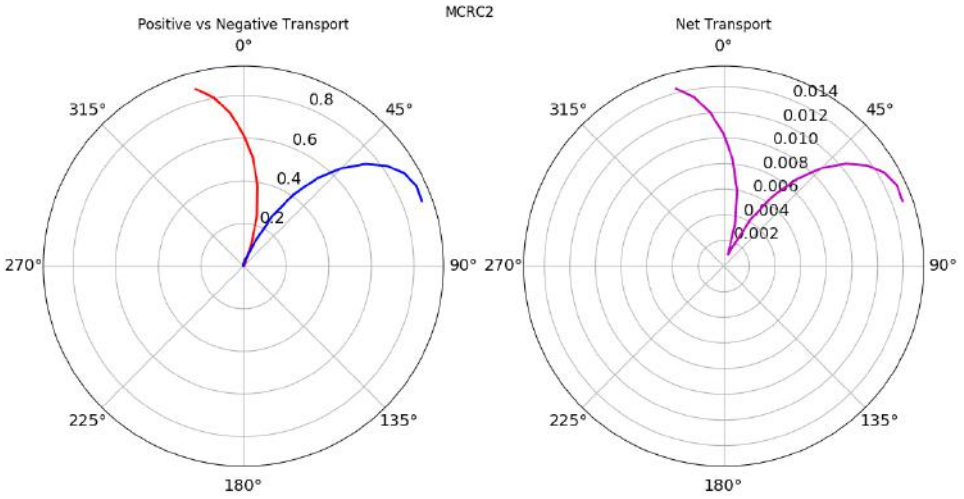

Figure 4.17: Wave sediment transport analysis over beach angles. Beach orientation is represented by the angle values and the transport is calculated for different wave directions. The left graph shows positive (blue line) and negative (red line) transport in millions cubic meters per year. The right graph shows the net transport in millions cubic meters per year per beach orientation.

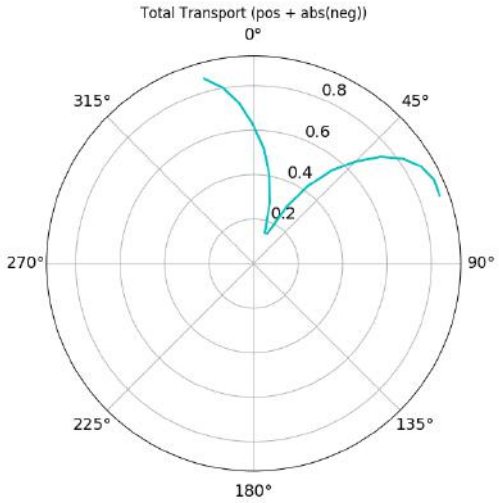

Figure 4.18: Total wave sediment transport analysis for Maçarico Beach in millions cubic meters per year per beach orientation. Total transport does not consider transport direction.

Figure 4.19 show a qualitative representation of the previous results. Considering beach orientation and wave climate, on the limit between Maçarico and Corvina, sediment transport direction diverges. On the adjacent area, there is a maximum value of sediment transport (represented by the red arrows on figure 4.19) forming a gradient of transport capacity.

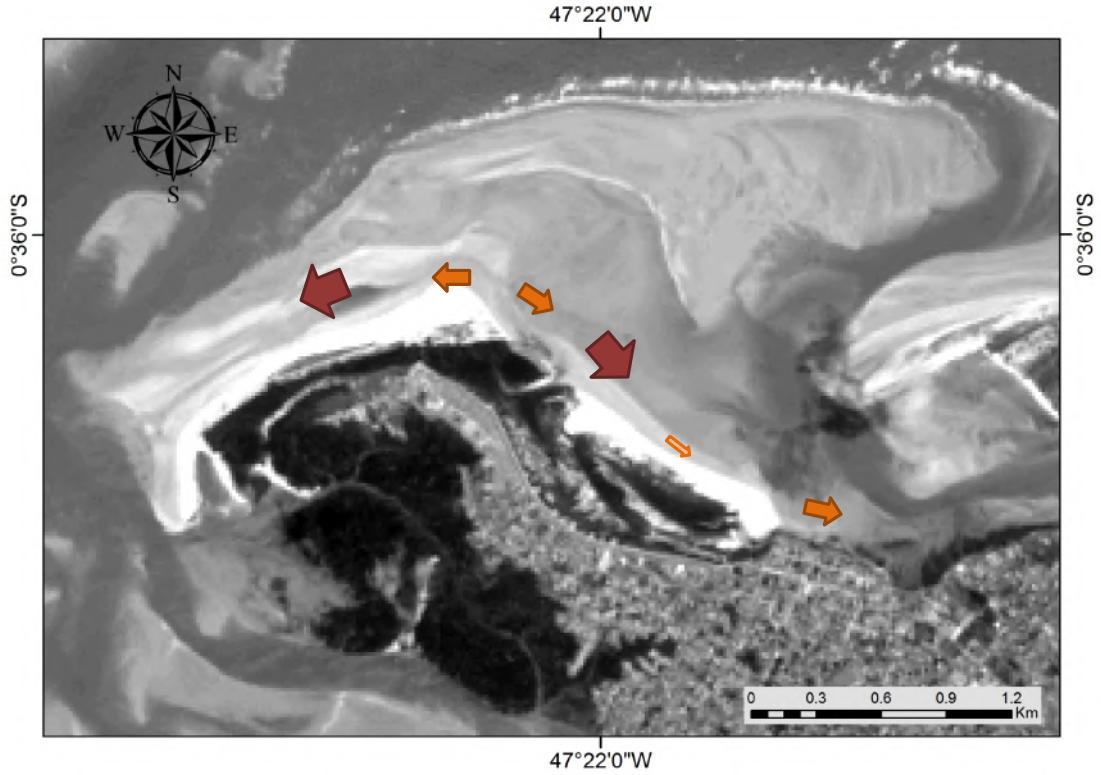

Figure 4.19: Sediment transport direction according to the results of wave sediment transport analysis. Arrows are a qualitative representation of the sediment transport result. The thin orange arrow represents the location of lower sediment transport; regular orange arrows represent intermediary values of transport and red arrows represent the location of maximum sediment transport.

4.6 Changes in Vegetation Area

Landsat 8 images were used in order to evaluate changes in vegetation line, representing the accretion of the beach. We compare the vegetation line changes with the 25-years analysis from RANIERI [28], and applied the same statistical calculation. A baseline was set parallel to the shorelines generating 65 transects 100 meters apart (Fig. 4.20).

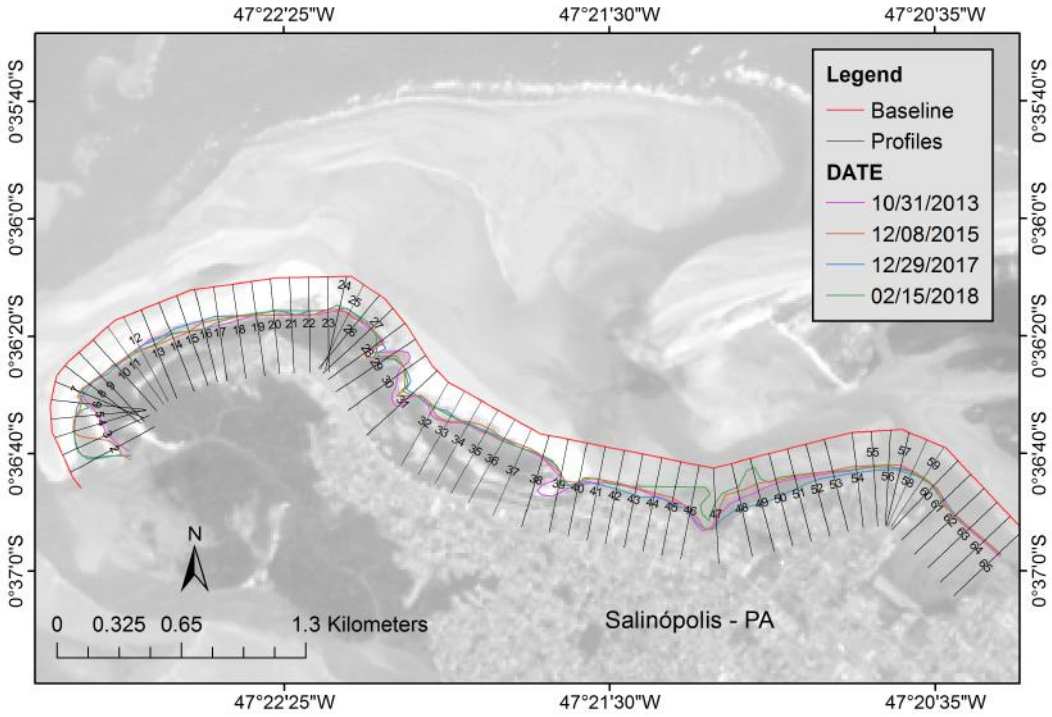

Figure 4.20: Shorelines(magenta, orange, blue and green), baseline (red) and the cross-sections (black) generated for statistical calculation of Maçarico and Corvina shoreline movement with DSAS.

The region presents an iner-annual dynamic with some significant coastline changes in a period of five years. One of the most significant change in coastline is the mangrove growth at the east portion of the beach (Fig. 4.20, transects 2 to 6) with a Net Shoreline Movement (NSM) of approximately 150 meters (Fig. 4.21).

NSM shows a tendency of accretion for the majority of transects (Fig. 4.21). Exceptions are transects 28 and 29 between Maçarico and Corvina with a negative NSM (shoreline regression) of -34.64 m (EPR -8.07 $m.yr^{-1}$) and -74.28 m (EPR -14.56 $m.yr^{-1}$), respectively (Fig. 4.22). At the corner between Corvina and Maçarico beaches (transects 24-29), RANIERI [28] observed an accretion of 40 $m.yr^{-1}$ between 1988 and 2001; and then an erosion of -10 $m.yr^{-1}$ from 2001 to 2013. From 2013 to 2018, a negative rate of -16 $m.yr^{-1}$ was registered at transect 28, located where today there is a tidal channel.

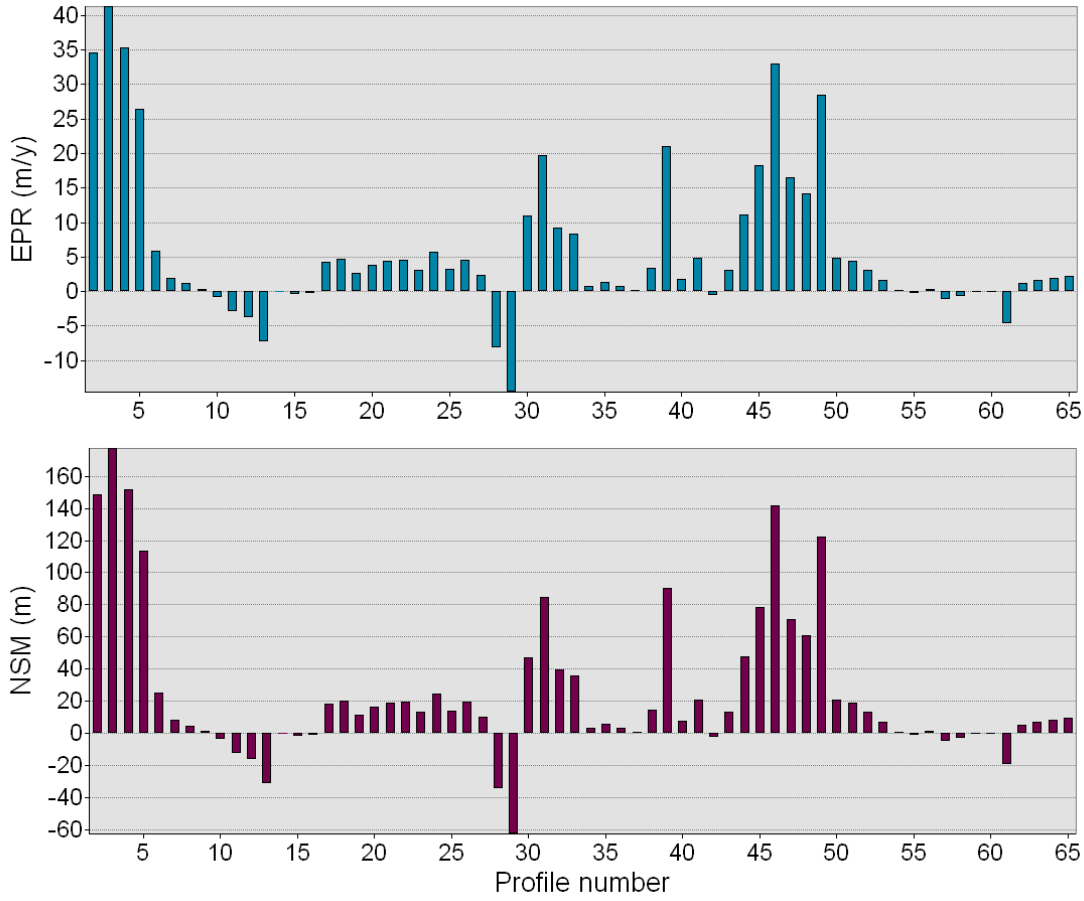

Figure 4.21: End Point Rate (top, blue bars) and Net Shoreline Movement (bottom, magenta bars) for each transect at Maçarico (transect 25 to 65) and Corvina (transect 2 to 24).

The mean NSM estimated for the period of 2013-2018 was 24.98 meters and the mean EPR was 5.81 meters per year (Fig. 4.21). For the period of 1988-2001 the mean EPR estimated was 18.24 $m.yr^{-1}$ and 4.61 $m.yr^{-1}$ for the period between 2001-2013 [28]. Taking into account that RANIERI [28] covered only the area from transect 7 to transect 40, mean EPR from 2013 to 2018 drop to only 2.52 $m.yr^{-1}$ almost half of the estimated rate for the period of 2001-2013.

Transects 40 to 46 are at the "Rua da Frente" extension. The concrete wall built at the beach extends from transect 40 to 43. At transects behind the concrete wall, accretion is significant smaller than at transects outside the wall influence (44 to 46 transects), where vegetation persists. The wall was partially destroyed by consistent small wave action and the cliff erosion persists. Although transects 40 to 49 shows significant accretion with NSM, year-to-year rate shows an alternation for erosion-accretion periods (Tab. 4.3). Transects 40-43 has low EPR with a maximum of 5 $m.yr^{-1}$ and a negative rate (-0.59 $m.yr^{-1}$) at transect 42.

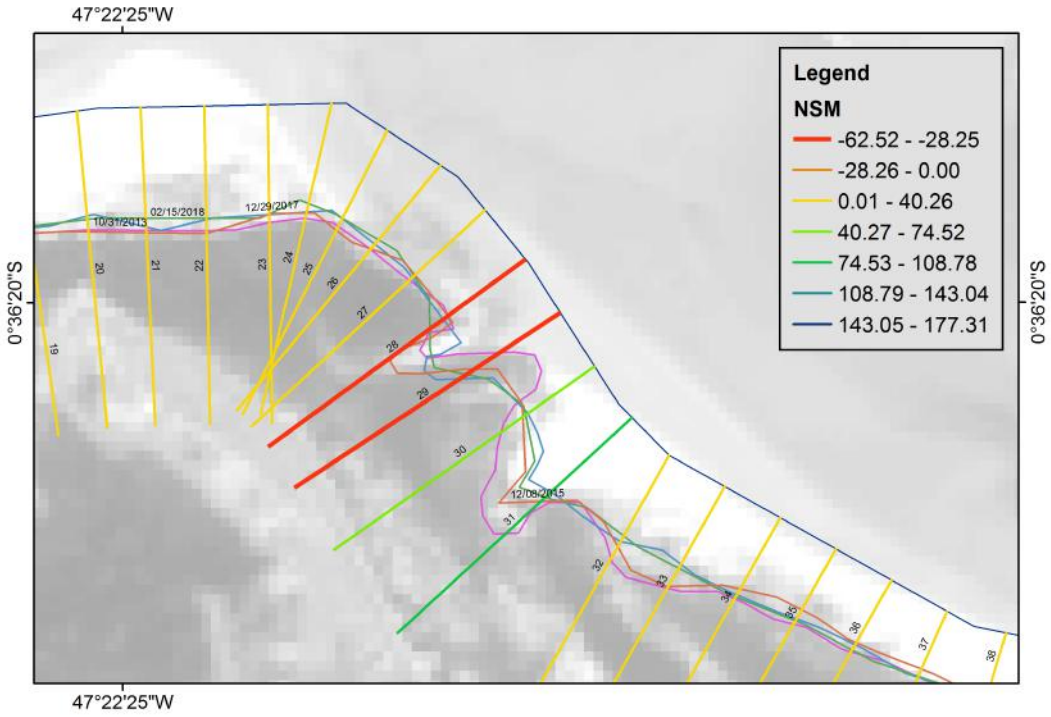

Figure 4.22: Zoom of the figure 4.20 at transects 19 to 37. Transects 28 and 29 between Maçarico and Corvina with a negative NSM are highlighted.

Table 4.3: Shoreline movement in 2013-2015; 2015-2017; 2017-2018. Negative values indicates erosion and positive values indicate accretion. Shoreline movement was calculated in meters.

Shoreline Movement (m)			
Transect	**2013-2015**	**2015-2017**	**2017-2018**
40	27.37	-10.96	-9.09
41	17.11	-24.68	28.40
42	8.70	-34.34	23.11
43	5.23	-38.00	45.83
44	13.26	-20.91	55.42
45	17.90	-33.01	93.58
46	24.40	-16.42	133.40
47	-28.56	-14.46	113.60
48	40.43	-90.98	111.42
49	35.13	-101.59	188.43

Chapter 5

Physical Framework for Tourism Development

Touristic activities based on beach recreation attracts visitors to Salinas in a defined seasonal distribution. Visiting is concentrated during summer break that coincides with the beginning of the dry season in July. However, the city has a larger potential developing other activities that would redistribute the number of tourists in a more homogeneous way throughout the year. The analysis of the physical parameters of Salinópolis aims to reinforce this potential and to stimulate a sustainable development of the city and a better engineering decision-making. The absence of available data for Pará coast, and other Brazilian sites as well, is often an obstacle for research and it was no different with this thesis. This is one of the reasons why engineering interventions and development decisions do not succeed. This section will summarize the main results presented on the previous chapter as well as discuss its application on practical actions.

5.1 Environmental Forcing and its Impacts on Tourist Activities

The most relevant factor for visitants decide to go to Salinas seems to be the rainfall climate. Precipitation volume varies significantly between wet, dry and transitional season. During the wet months (January-May) a mean value of 478 mm per month is registered, with 20 days of rain per month and the volume of rain being well distributed along the day. On the transitional period, an average of 125.65 $mm.month^{-1}$ is registered, three times less than the wet season. Dry season register an average of only 14.83 mm and less than 5 days of rain in a month (Sec. 4.2).

For a tourism based on beach activities, the second semester of the year is the

best period to visit Salinas. However, other activities independent on the weather could be developed and stimulated during the rest of the year. As an example of this is the gastronomic tourism, where the consumption of regional foods represents a significant motivation for the trip. Local food has an important role in visitors experience as an indispensable part of the traveling. Gastronomic tourists look for different tastes and memorable food and drink experiences during the trip and has become a popular way to interact with local culture [48–50].

Pará culture has a rich culinary of indigenous origin that uses mainly Amazonian ingredients [51]. Traditional dishes as duck with Tucupi and the Tacacá, as well as regional ingredients as the Açaí berry, the Cupuaçu and the Brazilian nuts are known internationally for its exotic flavors and health benefits [51]. As a coastal city, Salinópolis also has the tradition with fishery, serving dishes with crab, shrimp, oyster and fresh- or saltwater fishes. The culinary particularities of the region should be considered as a developing factor [51, 52]. An annual event calendar, including gastronomic and cultural events, can improve touristic activities during the low season and create a tradition for the city.

Aquatic sports like surfing and bodyboarding could benefit from less crowded beaches and higher waves that occurs during the first semester (Sec. 4.4). A flat sea is hardly seen in Salinas, even during the low wave season due to the persistence of trade winds in the region. During the wet season, waves reach their highest amplitude ranging from 0.8 m to 1.2 m. The presence of a long surf zone with multiples breaks is also an attractive characteristic. A well-succeeded surfing championship is already being promoted in Salinas showing the activity potential [53].

Surf industry has been growing since the emergence of the "Brazilian storm" in 2011, a reference to the Brazilian new surfer generation which has been standing out in the world surfing championship. The Brazilian Surf Institute (Ibrasurf) estimated in 2016 that surf industry movements R$ 7 billion per year with surf wear, board and accessories in Brazil. This amount increases if including expenses with hotel, feeding and transport during championships and other surf events that also promotes local tourism [54]. The industry does not only benefit from athletes but also from the created lifestyle that reaches the non-athletic public [54, 55].

The decrease in cumulative rainfall volume coincides with the increase of wind intensity in June (Sec. 4.1). Wind velocities reach 8 $m.s^{-1}$ throughout the year but wind mean velocity is higher during the second semester and culminating in September the strongest mean(Fig. 4.1). Wind intensity increases from 9 AM to 6 PM and a North component is also observed during this period (Fig. 4.3 and fig. 4.4). Those are signs from the breeze effect contribution.

Higher wind velocity, onshore or parallel to the coast and low rainfall volume is an interesting scenario for the practice of sail sports like kitesurfing and windsurfing.

Parallel and onshore winds bring security to the activity by making easier the return to the beach. The presence of different environments for the practice (exposed beaches with breaking waves and sheltered areas without obstacles, especially during low tide) attracts not only the more experienced athletes but also the beginners. Kitesurfing, the one with a kite controlled by strings, can be practiced with lower wind speed (10 knots or 5 $m.s^{-1}$) and has the size of the equipment - small and relative light - as an advantage to carry through the long distances of the beaches in Salinópolis. Windsurfing, the one with the sail attached to the board, needs stronger winds speed of at least 15 knots (almost 8 $m.s^{-1}$) and the equipment is heavier and bigger than kitesurf. The maximum wind speed observed in Salinópolis station is approximately 8 $m.s^{-1}$, the minimum necessary for the practice which makes kitesurfing a better option for the region.

5.2 Mangrove as a Touristic and Coastal Protection Feature

Besides infrastructure development and basic services implementation, Salinópolis also needs to preserve its natural resources since it is (or has potential to be) one of the tourist attraction of the city. White sandy beaches, dunes and mangrove forest more than aesthetics features are also natural coastal protection. Sand dunes act as sediment reservoir for the beach and mangrove forests protect the coastline attenuating wave energy.

Mangrove forest has the capacity to attenuate waves energy and trap sediment being a natural barrier against surges, storm waves and tsunamis. The devastation of this ecosystem caused erosion problems along the coast [56, 57]. Besides, mangrove forests have one of the greatest capacity for carbon storage [58, 59]. Tropical mangrove forest stocks about 103.7 tonne carbon per hectare ($tC.ha^{-1}$) on average only 25% less than rain forests and the mean carbon sequestration from mangrove forest (2.9 $tC.ha^{-1}.yr^{-1}$) is only slightly lower than in tropical rain forests (3.2 $tC.ha^{-1}.yr^{-1}$) [59]. In addition, preserving the mangrove forest is a way to sustain the gastronomic activity since some species are only found in this ecosystem and others use it as nursery.

There is a major portion of Salinópolis dominated by mangrove forests especially in areas close to the tidal channel and river mouths on the east and west portion of the study area. A mangrove forest has also developed between the promenade and the Maçarico and Corvina beaches restricting the access to the water. It is seen as a problem since it creates a barrier between the beach and the city, therefore hindering kiosks access and sea breeze in the city center.

Currently there is a North-South oriented concrete walkway through the mangrove that leads to the center of Maçarico beach (Fig. 1.2). This was built to solve the beach access problem but still there is a long walk until the water line and it does not minimize the airing problem. By knowing the main wind direction it is possible to optimize the design of a new walkway, constructing it parallel to the East and Northeast winds. A wider walkway could also permit the passage of bicycles and/or small motorized vehicles increasing mobility at the beach.

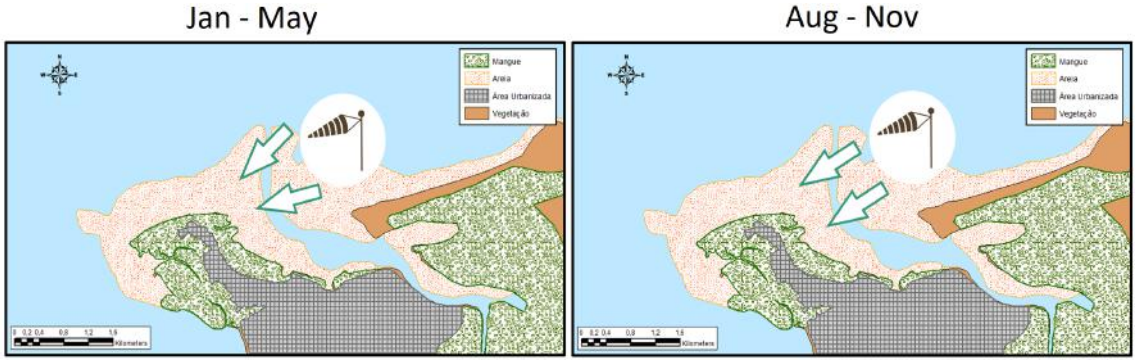

Figure 5.1: Wind major direction in relation to Maçarico and Corvina beaches for the period of January to May (on the left) and August to November (on the right)

The walkaways can be used to promote the eco-tourism. The installation of educational boards provide environmental information for visitors and guide birdwatch activities. This would aggregate educational and ecotouristic value to the walkways adding multiple functionalities without the necessity of devastating the forest.

Another important aspect of the project is to use wood instead of concrete in the walkways in order to make an easy to move structure that could be replaced or reconstructed. The predominant wind direction coincides with the incident wave angle and with a dynamic area in the mangrove at Maçarico beach (profiles 28 to 31 in figure 4.20), with annual shoreline variation and a divergent in sediment transport direction described in section 4.6 and section 4.5. In addition, wood walkways have an aesthetic idea of integration with nature. Examples of walkways made of wood can be observed in parks and beaches worldwide (Fig. 5.2). Recycled plastic that mimics wood would also be considered since the existence of Turú, a common mollusk that feeds on wood.

Accessibility and advanced birding infrastructure as trails and walkways are important to birdwatchers. This is shown by research from the Center for the Promotion of Imports from developing countries (CBI), part of the Netherlands Enterprise Agency [1]. Information boards on the biology of birds and their identification also add value to the paths and the use of educative board stimulates an environmental

[1] https://www.cbi.eu/market-information/tourism/birdwatching-tourism/

interaction for both visitors and residents.

A study from the Central Coast in Australia showed that tourists might not be aware of the environmental impacts of their activities and that an educational program is important to draw attention to the potential impacts associated regarding recreation activities in natural settings [60].

Figure 5.2: Walkways made of wood at (A) Siesta Beach, FL - United States; (B) and (C) Blue Springs National Park, FL - United States; (D) Mons Klint - Denmark; (E) Brisbane - Australia; (F) Krabi - Thailand. Pictures A to C are from personal archives and D to F were taken from Google research.

According to the US FISH AND WILDLIFE SERVICE [61], 17.8 millions of Americans travel the world to watch birds in their natural habitat and invest in the local community. Countries such as Austrália, United States and Canadá attract a select group of visitors with high scholarity and environmental conscience due to bird watch activities, a great stimulus to preserve local nature [62]. Some Brazilian states as Rio Grande do Sula, Paraná, Santa Catarina and Ceará also attract bird watchers [63]. According to the ICMCBIO [63], Salinópolis is a potential destiny for bird watch activities since it is part of the migratory route.

The littoral region of Pará and Maranhão concentrates more than 90% of the population of migratory species as *Arenaria interpres* (Turnstones or Vira-pedras), *Calidris pusilla* (Semipalmated sandpiper, Maçarico-Rasteirinho or Pilrito-

semipalmado), *Limnodromus griseus* (Short-billed Dowitcher or Maçarico-de-costas-brancas), *Numenius hudsonicus* (Hudsonian Curlew or Maçarico-de-bico-torto), *Pluvialis squatarola* (Grey Plover or Tarambola-cinzenta) and *Tringa semipalmata* (Willet or Maçarico-de-asa-branca), some of which are endangered species in Brazil [63]. The *Eudocimus ruber* (Scarlet Ibis or Guará vermelho) a symbol of Salinópolis, is commonly seen in the mangrove trees and feeds with crabs that live in the ecosystem.

Nevertheless, is very important to keep in mind the importance of mangrove forest preservation not only for touristic and economic activities but also as a coastal protection. Atalaia and Farol Velho beaches suffer from erosion problems as the sand stock from the dunes were no longer available after the construction of houses and hotels. The presence of protection structures like dikes and seawalls reduce properties prices while a natural coast with natural view increase accommodation value [64]. Hotel rooms with a beach view also increase their price in 10%-15% [65, 66].

Satellite images in addition to erosion observations and registers confirms the dynamic of Salinópolis coast. Although quantitative results from the sediment transport analysis might not be reliable due to the lack of data for the WALTON e DEAN [46] formula, qualitative results are very consistent with the satelite images analysis.

A cliff in the East side of Corvina beach - where there is a second access to the beach - was partially destroyed by erosive action. The area is sheltered from the big waves by the sand spit of Farol Velho. However, it is still under effect of small waves - that may promote as much erosion in fine sediment tidal flat as big waves, due to its high frequency [67]- combined with tidal currents as strong as 0.5 $m.s^{-1}$ (Fig. 4.10). Although the Net Shoreline Movement (NSM) at the cliff area shows significant accretion for the period from 2013 to 2018, annual rate shows an alternation between erosive/accretive periods (Tab. 4.3).

The area was isolated and a seawall was built as an attempt to stop erosion. However, the seawall was destroyed and erosion persisted (Fig. 1.3). The area where the seawall was had to be interdicted due to landslide danger. A cheaper and more effective tool to stop erosion would be to restore the mangrove forest that once existed there.

Mangrove restoration is not a simple task because of the very dynamic nature of the ecosystem, which experiences tidal flooding and strong tidal currents (Sec. 4.3) as well as other natural and anthropogenic disturbances [68]. Pioneer mangrove seeds need an ideal condition to establish on tidal flats such as protection from waves, currents and a period of inundation-free [69].

To restore the forest, a favorable environment for mangrove growth should be reconstructed as in Java, Indonesia, where a project uses natural materials such as bamboo and wood sticks to create permeable dams that trap fine sediments [57].

The project has a sustainable basement by using local materials and local labor as well as the idea of creating space for nature development (Fig. 5.3). In the absence of bamboo, local materials as Juta and Malva fibers could be used in the dams.

Figure 5.3: Permeable damns in Indonesia made with local labor and materials. Images kindly provided by prof. Susana Vinzón

Permeable dams as the one from Indonesia could be installed in front of the current seawall debris (at the corner of the "Rua da Frente"). This action would trap sediments, allow mangrove growth and protect the cliff against erosive processes. Results in section 4.6 show that the presence of vegetated areas are more effective on protecting coast against erosion than hard structures as the concrete seawall.

Chapter 6

Conclusion and Recommendations

The current tourism activities in Salinópolis are unsustainable. It has caused environmental problems that could have been mitigated by urban development planning policy [41]. The concentration of visitors during a restricted period of the year is also a source of environmental stress.

We conclude that Salinas has a touristic potential considering and protecting natural characteristics of the city. This potential is actually underexplored: for nautical sports, due to its wind climate and persistent wave action, and eco-turism activities with the possibility of building walkways in the accretive mangrove areas.

Responding to the specific research question it follows:

- Rainfall climatology using INMET and ANA data shows two well defined seasons: wet and dry, with a transitional period between them. Wind is constant over the year at Salinópolis but magnitude increases during the second semester. Wind blows parallel to the coast during the entire year. DELF3D hydrodynamic and wave models were used to propagate offshore wave for Salinas coastline. Model results agree with the available data. Waves are higher during the wet season, a good scenario for nautical sports like surfing.

- During the wet season, we proposed the development of cultural and gastronomical activities as they are less dependent on weather conditions. Gastronomic festivals and cultural events on specific months create a tradition for the city and attract visitors during low season. The first semester of the year is also the period when higher waves occurs and when regular championships could be done in order to discover new talents, attract the athletes and non-athletic public and promote the city. With the increase of wind velocity during the second semester we proposed to explore wind activities as sailing and kitesurfing classes and championships.

- Wind direction information would also be used to develop an ideal design for the mangrove walkways at Corvina and Maçarico. Walkways would have

multiple purpose as: improve mobility and access to those beaches; enhance airing circulation at the city center; provide environmental education to local and visitors and allow the development of birdwatching activities. Coastline movement analysis showed the importance of preserving mangrove as coastal protection ecosystem. Erosion at the cliff area ("Rua da Frente") would be reduced or stopped by creating an ideal environment where mangroves could recolonize, using local labor and low-cost material.

A sustainable and organized tourism growth would benefit local community, economy and the ecosystem. We expect that this thesis results could be used in order to provide a better management plan.

6.1 Recommendations for Future Works

As future works recommendations we would like to suggest actions that fill the major gap that is the lack of information, some development of the exposed ideas and the continuity of hydrodynamic model.

- Although model results were consistent with local observation, a nested grid should be run for a better resolution in Salinópolis;
- In order to calibrate the WALTON e DEAN [46] equation and reach a consistent sediment transport calculation, we suggest that local measures of longshore drift should be taken with this specific purpose;
- We suggest a specific study for the development of the permeable fences to determine its size and main direction. Tidal currents values and direction presented in this thesis might be used as base information;
- The approach on tourism activities should take social aspects of local population into account. We suggest this issue for future works in addition with the present thesis.

Bibliography

[1] BOSBOOM, J., STIVE, M. J. F. *Coastal Dynamics I*. VSSD, 2012. ISBN: 978-90-6562-286-0. Disponível em: <http://www.vssd.nl/hlf/019.htm>.

[2] VARIS, M. K., DE MOEL, H., SALVUCCI, G., et al. "Over the hills and further away from coast: global geospatial patterns of human and environment over the 20th-21st centuries", *Environmental Research Letters*, v. 11, n. 3, pp. 34010, 2016. ISSN: 1748-9326. doi: 10.1088/1748-9326/11/3/034010. Disponível em: <http://stacks.iop.org/1748-9326/11/i=3/a=034010>.

[3] SMALL, C., NICHOLLS, R. J. "A Global Analysis of Human Settlement in Coastal Zones", *Journal of Coastal Research*, v. 19, n. 3, pp. 584–599, 2003. ISSN: 07490208, 15515036. Disponível em: <http://www.jstor.org/stable/4299200>.

[4] IBGE. *Atlas geográfico das zonas costeiras e oceânicas do Brasil*. 2011. ISBN: 9788524042195. doi: 10.1017/CBO9781107415324.004.

[5] DAVENPORT, J., DAVENPORT, J. L. "The impact of tourism and personal leisure transport on coastal environments: A review", *Estuarine, Coastal and Shelf Science*, v. 67, n. 1-2, pp. 280–292, 2006. ISSN: 02727714. doi: 10.1016/j.ecss.2005.11.026.

[6] MOWFORTH, M., MUNT, I. *Tourism and Sustainablity: Development and New Tourism in the Third World*. Routledge, 2016. ISBN: 978–1–315–79534–8.

[7] COOPER, J. A. G., MCKENNA, J. "Boom and Bust: The Influence of Macroscale Economics on the World's Coasts", *Journal of Coastal Research*, v. 253, pp. 533–538, 2009. ISSN: 0749-0208. doi: 10.2112/09A-0001.1.

[8] KOMAR, P. D. *Beach Processes and Sedimentation*. Englewood Cliffs, New Jersey, Prentic-Hall, Inc., 1976. ISBN: 0-13-072595-1.

[9] MCKENNA, J., WILLIAMS, A. T., COOPER, J. A. G. "Blue Flag or Red Herring: Do beach awards encourage the public to visit beaches?" *Tourism Management*, v. 32, n. 3, pp. 576–588, 2011. ISSN: 02615177. doi: 10.1016/j.tourman.2010.05.005. Disponível em: <http://dx.doi.org/10.1016/j.tourman.2010.05.005>.

[10] GARCIA, C., SERVERA, J. "Impacts of Tourism Development on Water Demand and Beach Degradation on the Island of Impacts of Tourism Development on Water Demand and Beach Degradation on the Island of Mallorca (Spain)", *Tourism*, pp. 287–300, 2003. ISSN: 0435-3676. doi: 10.1111/j.0435-3676.2003.00206.x.

[11] BALDWIN, J. "Tourism development, wetland degradation and beach erosion in Antigua, West Indies", *Tourism Geographies*, v. 2, n. 2, pp. 193–218, 2000. doi: 10.1080/14616680050027897. Disponível em: <https://doi.org/10.1080/14616680050027897>.

[12] KABAT, P., BAZELMANS, J., VAN DIJK, J., et al. "The Wadden Sea Region: Towards a science for sustainable development", *Ocean and Coastal Management*, v. 68, pp. 4–17, 2012. ISSN: 09645691. doi: 10.1016/j.ocecoaman.2012.05.022. Disponível em: <http://dx.doi.org/10.1016/j.ocecoaman.2012.05.022>.

[13] HARRISON, DAVID, ., HITCHCOCK, M. *The politics of world heritage : negotiating tourism and conservation*. Clevedon, England : Channel View Publications, 2005. ISBN: 9781845410094 (hbk.).

[14] DE SOUZA, D. L. "Urbanização Turística, Políticas Públicas e Desenvolvimento: o caso de Salinópolis/PA", *Geografia em Questão*, v. 7, n. 1, pp. 65–86, 2014. doi: 21780234.

[15] DE SOUZA, D. L. *Produção do Espaço, Infraestrutura Turística e Desenvolvimento Sócio-Espacial: uma Análise do Complexo Orla do Maçarico e da Urbanização da Praia do Atalaia em Salinópolis-PA*. Dissertação (mestrado), Universidade Federal do Pará, 2014b.

[16] ALMEIDA, J. D. F. A., ALCÂNTARA NETO, C. P. "Ocupação e uso das Praias do Maçarico e das Corvinas (Salinópolis/PA): Subsídios á Gestão Ambiental", *Amazônia em Foco. Edição Especial: Empreendedorismo e Sustentabilidade*, , n. 1, pp. 160–178, 2013.

[17] IBGE. "Censo Demográfico de Salinópolis, PA". 2016. Disponível em: <http://cidades.ibge.gov.br/xtras/perfil.php?codmun=150620>.

[18] PORTAL DO SAL. "Conheça as badaladas noites de Salinas no mês de Julho". 2017. Disponível em: <http://portaldosal.com.br/2017/01/09/conheca-as-badaladas-noites-de-salinas-no-mes-de-julho/>.

[19] BATISTA, C. F. S., MAGALHÃES, R. D. C., BORGES, D. F. D. F. *Pesquisa de Turismo Receptivo: Demanda Turística do Município de Salinópolis*. Relatório técnico, CAXIUANÃ PLANEJAMENTO E GESTÃO EM TURISMO LTDA., 2008.

[20] GRUBER, A. "Fluctuations in the Position of the ITCZ in the Atlantic and Pacific Oceans", *Journal of the Atmospheric Sciences*, v. 29, pp. 193–197, 1972.

[21] UVO, C. R. B. *A zona de convergência intertropical (ZCIT) e sua relação com a precipitação na região Norte do Nordeste brasileiro*. Dissertação (mestrado), Instituto de Pesquisas Espaciais - INPE, 1989.

[22] XAVIER, T. D. M., XAVIER, A. F., DIAS, P. L. D. S., et al. "A ZONA DE CONVERGÊNCIA INTERTROPICAL - ZCIT E SUAS RELAÇÕES COM A CHUVA NO CEARÁ (1964-98)", *Revista Brasileira de Meteorologia*, v. 15, n. 1, pp. 27–43, 2000.

[23] CAVALCANTE SEGUNDO, G. H. *Processos Oceanográficos na Região Costeira e Estuarina do Rio Caeté, Pará, Brasil*. Doutorado em geoquímica ambiental, Universidade Federal Fluminense, 2007.

[24] SOUSA, R. C. D. C. *Considerações sobre a Interaçãa onda-corrente na Plataforma Continental Amazônica*. Tese de Doutorado, 2015.

[25] NOAA. "El Niño Southern Oscillation (ENSO)". Disponível em: <https://www.esrl.noaa.gov/psd/enso/>.

[26] SOUZA, E. B. D., KAYANO, M. T., TOTA, J., et al. "On the influences of the El Niño, La niña and Atlantic Dipole Paterni on the Amazonian Rainfall during 1960-1998", *Acta Amazonica*, v. 30, pp. 305 – 318, 06 2000. ISSN: 0044-5967. Disponível em: <http://www.scielo.br/scielo.php?script=sci_arttext&pid=S0044-59672000000200305&nrm=iso>.

[27] DIRETORIA NACIONAL DE HIDROGRAFIA. "Cartas de Correntes de Salinópolis a Belém". 1962. Disponível em: <https://www.mar.mil.br/dhn/chm/box-publicacoes/publicacoes/ccm/CCM-Salinopolis-a-Belem.pdf>.

[28] RANIERI, L. A. *Morfodinâmica Costeira e o Uso da Orla Oceânica de Salinópolis (Nordeste Do Pará , Brasil).* Tese de doutorado, Universidade Federal do Pará, 2014.

[29] PEREIRA, L. C. C., PINTO, K. S. T., VILA-CONCEJO, A. "Morphodynamic variations of a macrotidal beach (Atalaia) on the Brazilian Amazon Coast", *Journal of Coastal Research*, , n. 70, pp. 681–686, 2014.

[30] RANIERI, L. A., EL-ROBRINI, M. "Correntes Nas Praias Oceânicas De Salinópolis , Nordeste", v. 2, n. 1, 2016.

[31] PEREIRA, L. C. C., VILA-CONCEJO, A., SHORT, A. D. "Influence of subtidal sand banks on tidal modulation of waves and beach morphology in Amazon macrotidal beaches." *Journal of Coastal Research*, v. SI 65, n. Special Issue Proceedings 12th International Coastal Symposium (Plymouth, England), pp. 1821–1826, 2013. ISSN: 0749-0208. doi: 10.2112/SI65-308.1.

[32] CERC. *SHORE PROTECTION MANUAL*, v. v. 1. 4th ed. ed. Vicksburg, Mississipi, 1984. doi: 10.5962/bhl.title.47830. Disponível em: <http://scholar.google.com/scholar?hl=en{&}btnG=Search{&}q=intitle:Shore+Protection+Manual{#}0>.

[33] HANLEY, M. E., HOGGART, S. P. G., SIMMONDS, D. J., et al. "Shifting sands? Coastal protection by sand banks, beaches and dunes", *Coastal Engineering*, v. 87, pp. 136–146, 2014. ISSN: 03783839. doi: 10.1016/j.coastaleng.2013.10.020. Disponível em: <http://dx.doi.org/10.1016/j.coastaleng.2013.10.020>.

[34] FISCH, C. I. *Caracterização do clima de ondas na costa do Ceará*. Dissertação, Universidade Federal do Rio de Janeiro, 2008.

[35] EL-ROBRINI, M., SILVA, M. M. A. D., SOUZA FILHO, P. W. M., et al. "Pará". In: *Erosão e progradação do litoral brasileiro*, pp. 41–86, 2005.

[36] GREGÓRIO, A. M. D. S., MENDES, A. C., BUSMAN, D. V. "Morfodinâmica da Praia do Atalaia, Salinópolis - Pará." In: *Anais do X Congresso da Associação Brasileira de Estudos do Quaternário*, pp. 153–168, Guarapari, 2005.

[37] ADRIÃO, D. "Pescadores de Sonhos: um olhar sobre as mudanças nas relações de trabalho e na organização social entre as famílias dos pescadores diante do veraneio e do turismo balnear em Salinópolis,

Pará", *Boletim do Museu Paraense Emílio Goeldi. Ciências Humanas*, v. 1, n. 2, pp. 11–21, 2006. doi: 10.1590/S1981-81222006000200002. Disponível em: <http://goo.gl/L5PXl{%}5Cnhttp://www.scielo.br/pdf/bgoeldi/v1n2/v1n2a02.pdf>.

[38] ABREU, M. M. O., VEIGA, N., COSTA-NETO, S. V., et al. "Vegetação Arbórea: Distribuição Espacial". In: Fernandes, M. E. B. (Ed.), *Os Manguezais da Costa Norte Brasileira Vol. III*, p. 175, Bragança: Laboratório de Ecologia de Manguezal, 2016. ISBN: 9788589547031.

[39] ARAÚJO JÚNIOR, A. C. R. "MANGUEZAL COMO EXPRESSÃO DA PAISAGEM GEOGRÁFICA NA CIDADE DE SALINÓPOLIS (PA)", *Revista Casa da Geografia de Sobral*, v. 19, n. 2, pp. 3–20, dec 2017.

[40] RANIERI, L. A., EL-ROBRINI, M. "Evolução da linha de costa de Salinópolis, Nordeste do Pará, Brasil", *Pesquisas em Geociencias*, v. 42, n. 3, pp. 207–226, 2015. ISSN: 18079806.

[41] ASSUNÇÃO, F. P., MATTA, M. A. D. S., SILVA, L. S., et al. "PROBLEMAS AMBIENTAIS DA OCUPAÇÃO URBANA DE SALINÓPOLIS – PARÁ E SUA INFLUÊNCIA NO ABASTECIMENTO DE ÁGUA LOCAL". In: *XVII Congresso Brasileiro de Águas SUbterrâneas*, pp. 1–4, 2012.

[42] THIELER, E., HIMMELSTOSS, E., ZICHICHI, J., et al. "The Digital Shoreline Analysis System (DSAS) version 4.0—an ArcGIS Extension for Calculating Shoreline Change (ver. 4.4, July 2017)", *U.S. Geological Survey Open-File Report 2008-1278*, 2017. Disponível em: <https://woodshole.er.usgs.gov/project-pages/DSAS/version4/index.html>.

[43] DEE, D. P., UPPALA, S. M., SIMMONS, A. J., et al. "The ERA-Interim reanalysis: Configuration and performance of the data assimilation system", *Quarterly Journal of the Royal Meteorological Society*, v. 137, n. 656, pp. 553–597, 2011. ISSN: 00359009. doi: 10.1002/qj.828.

[44] DELTARES. *Delft3D-WAVE*. N. May. Version 3. ed. Delft, Deltares, 2011.

[45] DELTARES. "Delft Dashboard: a MATLAB- based rapid tool for setting up coastal and estuarine models", pp. 1–64, 2016. Disponível em: <https://publicwiki.deltares.nl/display/DDB/General>.

[46] WALTON, T. L., DEAN, R. G. "Longshore sediment transport via littoral drift rose", *Ocean Engineering*, v. 37, n. 2-3, pp. 228–235, 2010. ISSN:

00298018. doi: 10.1016/j.oceaneng.2009.11.002. Disponível em: <http://dx.doi.org/10.1016/j.oceaneng.2009.11.002>.

[47] CEM. "Part III: Chapter 1 - Coastal Sediment Properties". In: *Coastal Engineering Manual*, v. 1100, pp. III–1–1 to III–1–41, 2002. ISBN: EC 1110-2-292.

[48] GÜZEL, B. "Gastronomy Tourism: Motivations and Destinations", , n. January 2016, pp. 394–404, 2016.

[49] SENGEL, T., KARAGOZ, A., CETIN, G., et al. "Tourists' Approach to Local Food", *Procedia - Social and Behavioral Sciences*, v. 195, n. 2013, pp. 429–437, 2015. ISSN: 18770428. doi: 10.1016/j.sbspro.2015.06.485. Disponível em: <http://linkinghub.elsevier.com/retrieve/pii/S1877042815039646>.

[50] GHEORGHE, G., TUDORACHE, P., NISTOREANU, P. "Gastronomic Tourism, a New Trend for Contemporary Tourism??" *Cactus Tourism Journal*, v. 9, n. 1, pp. 1221, 2014.

[51] QUINZANI, S. S. P., CAPOVILLA, V. M., CORRÊA, A. A. "A PLURALIDADE GASTRONÔMICA DA REGIÃO AMAZÔNICA: sabores acreanos, paraenses e do Alto Rio Negro", *Rev Hospitalidade*, v. 13, pp. 248–271, 2016.

[52] SORMAZ, U., AKMESE, H., GUNES, E., et al. "Gastronomy in Tourism", *Procedia Economics and Finance*, v. 39, n. November 2015, pp. 725–730, 2016. ISSN: 22125671. doi: 10.1016/S2212-5671(16)30286-6. Disponível em: <http://linkinghub.elsevier.com/retrieve/pii/S2212567116302866>.

[53] ESPORTE, G. "Salinas recebe a I etapa do Circuito Brasileiro de Surf 2017 nesta semana". 2017. Disponível em: <http://globoesporte.globo.com/pa/noticia/2017/03/salinas-recebe-i-etapa-do-circuito-brasileiro-de-surf-2017=nesta-semana.html>.

[54] NETO, J. S. "Surfe movimenta R$ 7 bi ao ano em roupas, pranchas e acessórios". 2016. Disponível em: <https://oglobo.globo.com/economia/surfe-movimenta-7-bi-ao-ano-em-roupas-pranchas-acessorios=20547660>.

[55] DINIZ, P. "Bom desempenho de brasileiros do surfe estimula consumo associado ao estilo". 2016. Disponível em: <http://www1.folha.uol.com.br/mercado/2016/06/1785587-bom-desempenho-brasileiros-do-surfe-estimula-consumo=associado-ao-estilo.shtml>.

[56] VISWANATHAN, P. K. "Conservation, Restoration, and Management of Mangrove Wetlands Against Risks of Climate Change and Vulnerability of Coastal Livelihoods in Gujarat". In: Nautiyal, S., Rao, K. S., Kaechele, H., et al. (Eds.), *Knowledge Systems of Societies for Adaptation and Mitigation of Impacts of Climate Change*, pp. 423–441, Berlin, Heidelberg, Springer Berlin Heidelberg, 2013. ISBN: 978-3-642-36143-2. doi: 10.1007/978-3-642-36143-2_25. Disponível em: <https://doi.org/10.1007/978-3-642-36143-2{_}25>.

[57] VAN WESENBEECK, B. K., BALKE, T., VAN EIJK, P., et al. "Aquaculture induced erosion of tropical coastlines throws coastal communities back into poverty", *Ocean and Coastal Management*, v. 116, pp. 466–469, 2015. ISSN: 09645691. doi: 10.1016/j.ocecoaman.2015.09.004.

[58] DONATO, D. C., KAUFFMAN, J. B., MURDIYARSO, D., et al. "Mangroves among the most carbon-rich forests in the tropics", *Nature Geoscience*, v. 4, pp. 293, apr 2011. Disponível em: <http://dx.doi.org/10.1038/ngeo1123http://10.0.4.14/ngeo1123https://www.nature.com/articles/ngeo1123{#}supplementary-information>.

[59] ESTRADA, G. C. D., SOARES, M. L. "Global patterns of aboveground carbon stock and sequestration in mangroves", *Anais da Academia Brasileira de Ciencias*, v. 89, n. 2, pp. 973–989, 2017. ISSN: 16782690. doi: 10.1590/0001-3765201720160357.

[60] PRISKIN, J. "Tourist perceptions of degradation caused by coastal nature-based recreation", *Environmental Management*, v. 32, n. 2, pp. 189–204, 2003. ISSN: 0364152X. doi: 10.1007/s00267-002-2916-z.

[61] US FISH AND WILDLIFE SERVICE. "2011 National Survey of Fishing, Hunting, and Widllife-associated Recreation", , n. August, 2012.

[62] KERLINGER, P., BRETT, J. "Hawk Mountain Sanctuary: A Case Study of Birder Visitation and Birding Economics". In: Knight, R. L., Gutzwiller, K. J. (Ed.), *Wildlife and Recreationists: Coexistence Through Management and Research*, Island Press,

cap. Chapter 16, 1995. ISBN: 1-55963-258-5. Disponível em: <https://s3.amazonaws.com/academia.edu.documents/39184559/6fb3a955838dd225f4a1d745926052ca.pdf?AWSAccessKeyId=AKIAIWOWYYGZ2Y53UL3A{&}Expires=1510407562{&}Signature=j27npHYqbMDJ8Qp7TYJmKc{%}2ByNLY{%}3D{&}response-content-disposition=inline{%}3Bfilename{%}3DWildlife{_}and{_}>.

[63] ICMCBIO. "Relatório Anual de Rotas e Áreas de Concentração de aves migratórias no Brasil", *CEMAVE/ICMBio*, p. 87, 2016. ISSN: 08628408. doi: 10.1007/s13398-014-0173-7.2.

[64] HAMILTON, J. M. "Coastal landscape and the hedonic price of accommodation", *Ecological Economics*, v. 62, n. 3-4, pp. 594–602, 2007. ISSN: 09218009. doi: 10.1016/j.ecolecon.2006.08.001.

[65] RIGALL-I-TORRENT, R., FLUVIÀ, M., BALLESTER, R., et al. "The effects of beach characteristics and location with respect to hotel prices", *Tourism Management*, v. 32, n. 5, pp. 1150–1158, 2011. ISSN: 02615177. doi: 10.1016/j.tourman.2010.10.005. Disponível em: <http://dx.doi.org/10.1016/j.tourman.2010.10.005>.

[66] FLEISCHER, A. "A room with a view-A valuation of the Mediterranean Sea view", *Tourism Management*, v. 33, n. 3, pp. 598–602, 2012. ISSN: 02615177. doi: 10.1016/j.tourman.2011.06.016. Disponível em: <http://dx.doi.org/10.1016/j.tourman.2011.06.016>.

[67] WINTERWERP, J. C., BORST, W. G., DE VRIES, M. B. "Pilot Study on the Erosion and Rehabilitation of a Mangrove Mud Coast", *Journal of Coastal Research*, v. 212, pp. 223–230, 2005. ISSN: 0749-0208. doi: 10.2112/03-832A.1. Disponível em: <http://www.bioone.org/doi/abs/10.2112/03-832A.1>.

[68] BISWAS, S. R., MALLIK, A. U., CHOUDHURY, J. K., et al. "A unified framework for the restoration of Southeast Asian mangroves—bridging ecology, society and economics", *Wetlands Ecology and Management*, v. 17, n. 4, pp. 365–383, 2009. ISSN: 1572-9834. doi: 10.1007/s11273-008-9113-7. Disponível em: <https://doi.org/10.1007/s11273-008-9113-7>.

[69] BALKE, T., TJ, B., EM, H., et al. "Windows of opportunity: thresholds to mangrove seedling establishment on tidal flats ", *Marine Ecology Progress Series*, v. 440, pp. 1–9, 2011. Disponível em: <http://www.int-res.com/abstracts/meps/v440/p1-9/>.